



SMR: 1643/10

**WINTER COLLEGE ON OPTICS ON OPTICS AND PHOTONICS
IN NANOSCIENCE AND NANOTECHNOLOGY**

(7 - 18 February 2005)

***"Optical Response of Semiconductor
Quantum Dots"***

presented by:

G. Cassabois

Laboratoire Pierre Aigrain

Paris

France

These are preliminary lecture notes, intended only for distribution to participants.

Optical response of semiconductor quantum dots

G. Cassabois

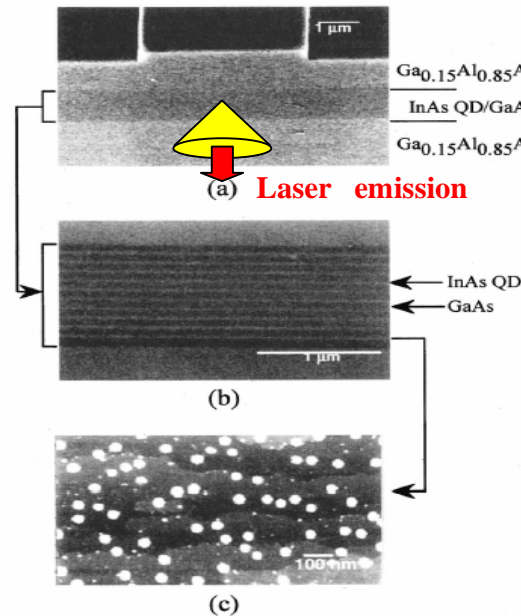
Laboratoire Pierre Aigrain - Ecole Normale Supérieure - Paris

Outline

- fundamental optical properties
- single-photon emission
- spontaneous emission control



Doing optics with quantum dots



Nakamura
J. Appl. Phys. **94**, 1184 (2003)

QD laser

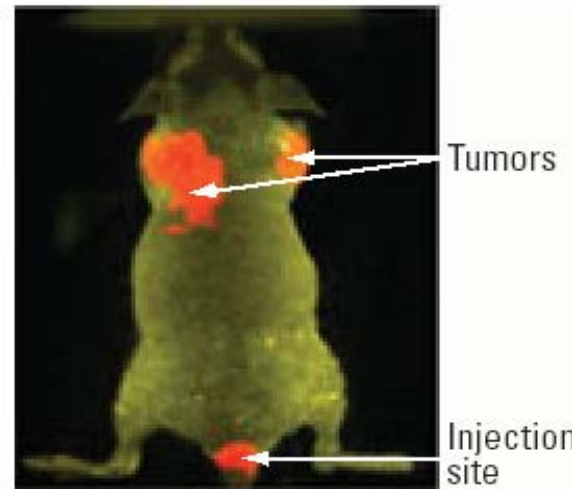
Opto-electronics



Bio-physics

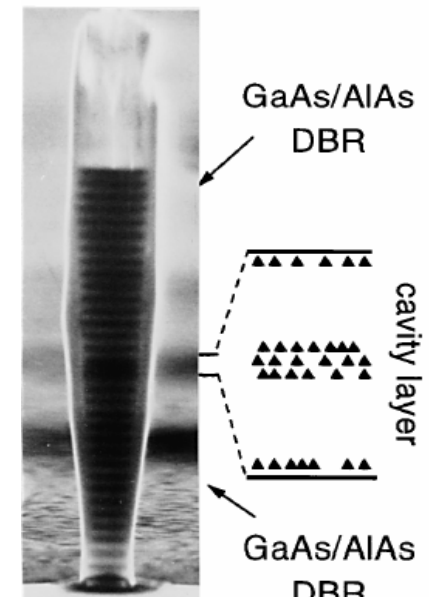
Biological sensors

In vivo imaging of cancer cells in a living mouse



Gao, Nature Biot. **22**, 969 (2004)

1 μm

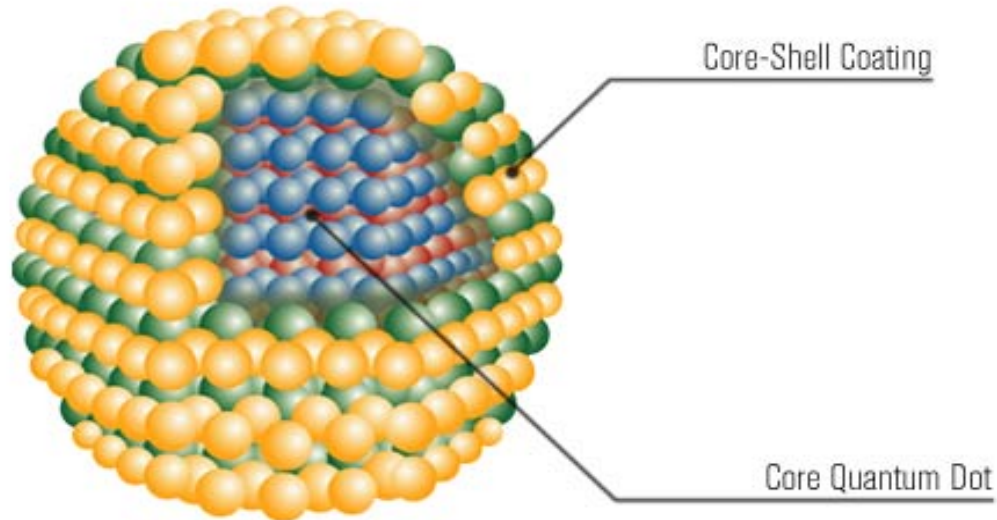


Gérard, PRL **81**, 1110 (1998)

Single photon source

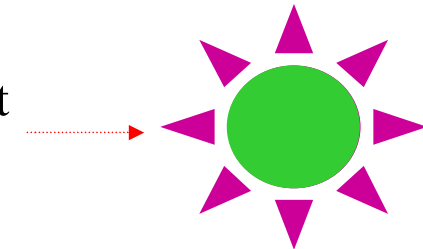
Quantum optics

Colloidal QD



- **Chemically synthesized** quantum dots in colloids (charged particles, inverse micelle)

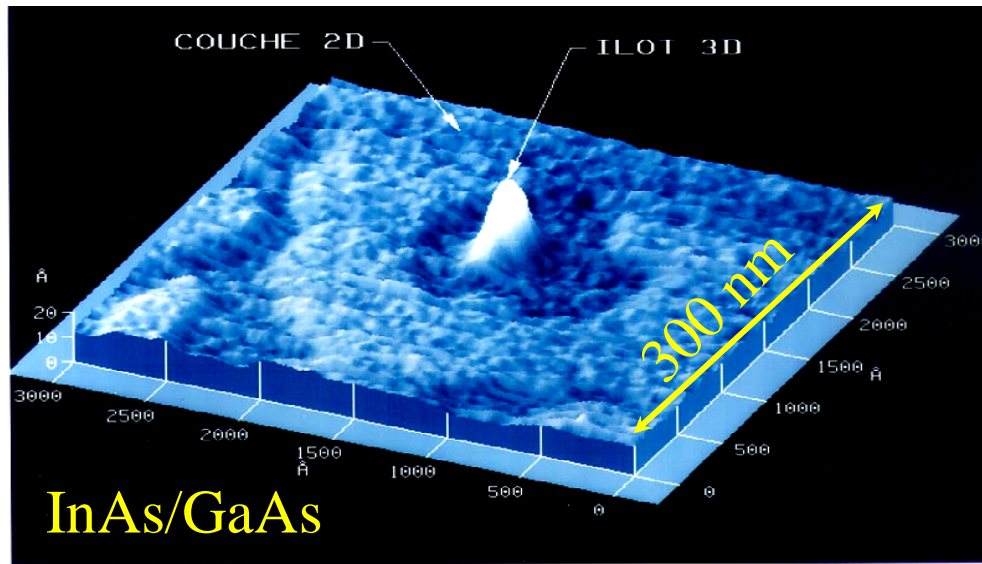
surfactant
molecule



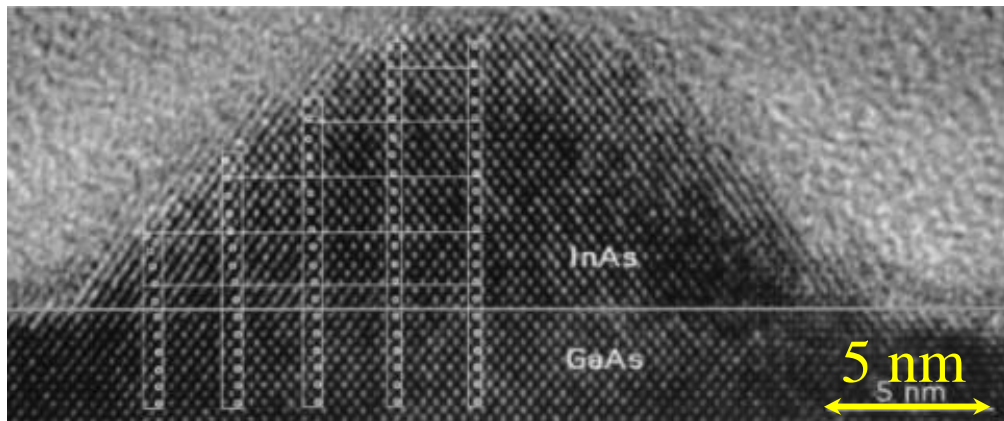
- **Core** material : CdS, CdSe, CdTe
- **Core-Shell** structure
 - surface passivation
 - suppression of non-radiative decay channels
- **Bio-conjugation** of QD with adequate coating



Epitaxially grown QD



J. M. Gérard *et al.*, J. Cryst. Growth **150**, 351 (1995)



- Molecular Beam Epitaxy
- Self-assembled quantum dots with areal density $< 10^3 \mu\text{m}^{-2}$
- Stranski-Krastanow growth mode
 - strain accumulation because of lattice mismatch
 - critical thickness of wetting layer ~ 1.7 monolayer for InAs
 - spontaneous formation of pyramids
- various systems : InAs/GaAs, InAs/InP, Ge/Si, GaN/AlN, CdTe/MnTe, CdSe/ZnSe ...



<http://www.wsi.tum.de/E24/research/nanostructures/>

Fundamental optical properties

Outline

- light-matter interaction
- interband and intraband transitions
- single QD spectroscopy
- specific solid-state features



Light-matter interaction

- Single particle Hamiltonian of an electron in a crystal reads

$$H_0 = \frac{\vec{p}^2}{2m} + V(\vec{r})$$

- Interaction of an electron with an electromagnetic field is obtained from **generalized impulsion**

$$\vec{p}' = m\vec{v}' - e\vec{A} \quad (\text{Lagrangian mechanics})$$

- Single particle Hamiltonian becomes

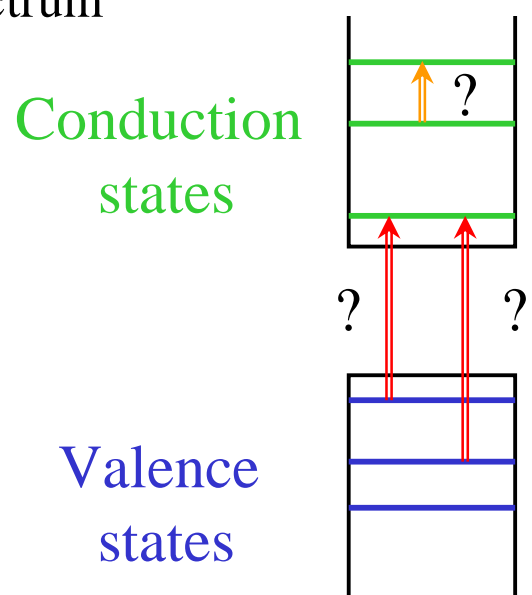
$$\begin{aligned} H &= \frac{(\vec{p}' + e\vec{A})^2}{2m} + V(\vec{r}) \\ &= \underbrace{\frac{\vec{p}'^2}{2m} + V(\vec{r})}_{H_0} + \underbrace{\frac{e}{2m}(\vec{p}' \cdot \vec{A} + \vec{A} \cdot \vec{p}')}_{\text{dipole interaction}} + \underbrace{\frac{e\vec{A}^2}{2m}}_{\text{diamagnetic shift}} \end{aligned}$$

the **second term** simplifies because $\vec{p}' \cdot \vec{A} - \vec{A} \cdot \vec{p}' = \frac{\hbar}{i} \operatorname{div} \vec{A} = 0$
(Coulomb gauge)



Dipole interaction

- Optical transitions between electronic states $|i\rangle \rightarrow |f\rangle$ induced by the dipole interaction term $H_I = \frac{e}{m}(\vec{A} \cdot \vec{p})$
- Their strength depends on the matrix element $\langle f | H_I | i \rangle$
- In semiconductor QDs, the 3D confinement leads to a discrete electronic spectrum



One expects an absorption spectrum formed by a set of discrete lines

What are the selection rules ?

$$\langle f | H_I | i \rangle \neq 0$$



Envelope function approximation

- In the envelope function approximation, electron wave-functions are given by

$$\psi_\alpha(\vec{r}) = \phi_\alpha(\vec{r}) u_\alpha(\vec{r})$$

slowly varying envelope function periodic rapidly varying atomic function

The diagram shows a yellow sphere labeled "quantum dot" with a diameter $D \sim \text{few nm}$. To its right is a 3D cube divided into smaller cubes, labeled "unit cell Ω_0 " with a side length $d \sim \text{few \AA}$.

- Matrix element $\langle f | H_I | i \rangle \sim \frac{e}{m} \vec{A} \cdot \langle f | \vec{p} | i \rangle$ (Long wavelength approx.)

$$\sim \frac{e}{m} \vec{A} \cdot \int d\vec{r} \phi_f^*(\vec{r}) u_f^*(\vec{r}) \vec{p}(\phi_i(\vec{r}) u_i(\vec{r}))$$

$$\sim \frac{e}{m} \vec{A} \cdot \int d\vec{r} \phi_f^*(\vec{r}) u_f^*(\vec{r}) u_i(\vec{r}) \vec{p}(\phi_i(\vec{r}))$$

2 terms

$$+ \frac{e}{m} \vec{A} \cdot \int d\vec{r} \phi_f^*(\vec{r}) u_f^*(\vec{r}) \phi_i(\vec{r}) \vec{p}(u_i(\vec{r}))$$



Intraband and interband transitions

$$\begin{aligned}\langle f | H_I | i \rangle &\sim \frac{e}{m} \vec{A} \cdot \int d\vec{r} \phi_f^*(\vec{r}) \vec{p}(\phi_i(\vec{r})) \cdot \frac{1}{\Omega_0} \int_{\Omega_0} d\vec{r} u_f^*(\vec{r}) u_i(\vec{r}) = \text{(1)} \\ &+ \frac{e}{m} \vec{A} \cdot \int d\vec{r} \phi_f^*(\vec{r}) \phi_i(\vec{r}) \cdot \frac{1}{\Omega_0} \int_{\Omega_0} d\vec{r} u_f^*(\vec{r}) \vec{p}(u_i(\vec{r})) = \text{(2)}\end{aligned}$$

- These two terms can be rewritten as:

$$\begin{aligned}\langle f | H_I | i \rangle &\sim \frac{e}{m} \vec{A} \cdot \langle \phi_f | \vec{p} | \phi_i \rangle \cdot \langle u_f | u_i \rangle = \text{(1)} \\ &+ \frac{e}{m} \vec{A} \cdot \langle \phi_f | \phi_i \rangle \cdot \langle u_f | \vec{p} | u_i \rangle = \text{(2)}\end{aligned}$$

- The first term **(1)** accounts for **INTRABAND** transitions

if $u_f = u_i = u_c$ or $u_f = u_i = u_v$ then $\langle u_f | \vec{p} | u_i \rangle = 0$

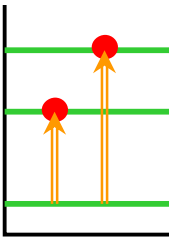
- The second term **(2)** accounts for **INTERBAND** transitions

if $u_f \neq u_i$ then $\langle u_f | u_i \rangle = 0$



Intraband transitions

$$P_{|i\rangle \rightarrow |f\rangle} = \frac{2\pi}{\hbar} \left| \frac{e}{m} \vec{A} \cdot \langle \phi_f | \vec{p} | \phi_i \rangle \right|^2 \delta(E_f - E_i - \hbar\omega)$$

Conduction states 

Valence states 

Only electrons Only holes

or

Polarization of incident electromagnetic field Energy conservation

- Absorption in $\begin{cases} \text{energy range of } & 10-100 \text{ meV} \\ \text{wavelength range of } & 10-100 \mu\text{m} \end{cases}$
Mid-Long IR
- Assumption of initial state occupied
and final state empty

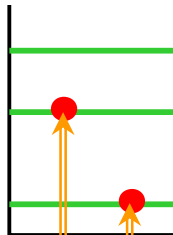
QDs must be doped



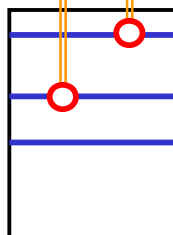
Interband transitions

$$P_{|i\rangle \rightarrow |f\rangle} = \frac{2\pi}{\hbar} \left| \frac{e}{m} \cdot \underbrace{\langle \phi_f | \phi_i \rangle}_{\text{Parity selection rule}} \cdot \overrightarrow{A} \cdot \underbrace{\langle u_f | \vec{p} | u_i \rangle}_{\text{Polarization selection rule}} \right|^2 \underbrace{\delta(E_f - E_i - \hbar\omega)}_{\text{Energy conservation}}$$

Conduction states



Valence states

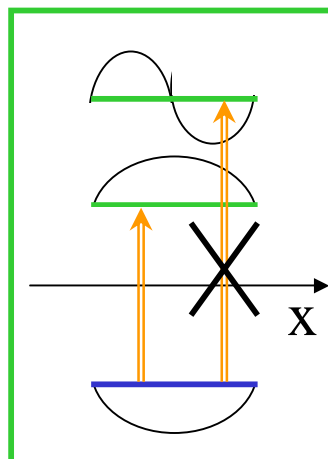


Electron AND hole

Parity selection rule

Polarization selection rule

Energy conservation



• Absorption in

Circularly polarized light propagating along (Oz), couples electronic states

$$\Delta J_z = +/ - 1$$

In zinc-blende type semiconductors,

$$| \text{electron} \rangle = | J = 1/2, J_z = \pm 1/2, \dots \rangle$$

$$| \text{heavy hole} \rangle = | J = 3/2, J_z = \pm 3/2, \dots \rangle$$

$$| \text{light hole} \rangle = | J = 3/2, J_z = \pm 1/2, \dots \rangle$$

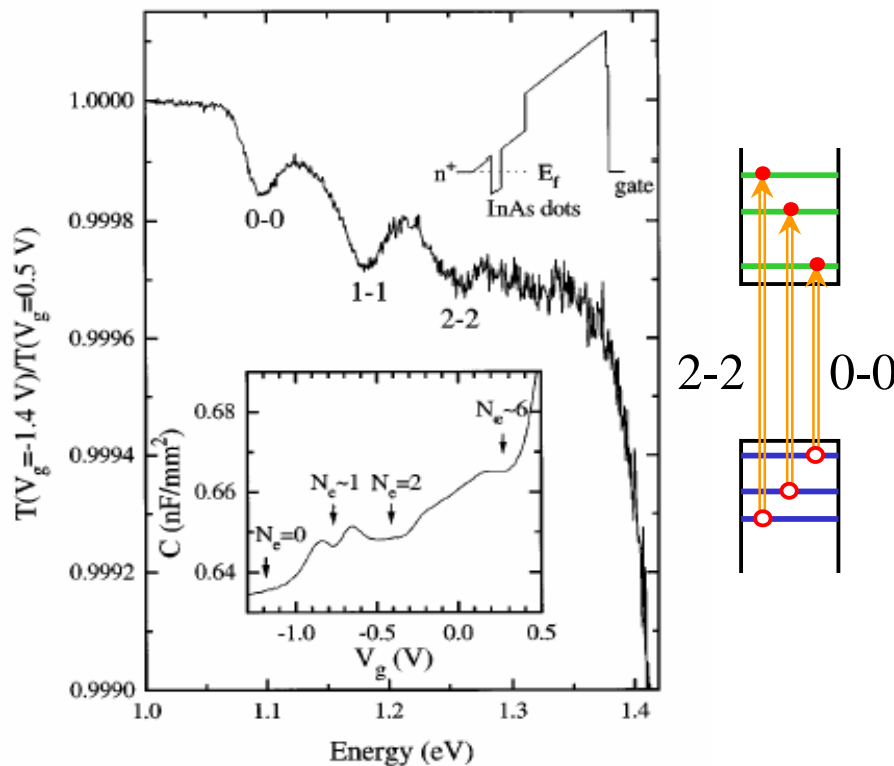
energy range of 1 - 2.5 eV
 wavelength range of 0.4 - 1 μm

Visible -NIR



Interband absorption spectroscopy

Transmission experiment
in an ensemble of InAs QDs



Warburton, PRL **79**, 5282 (1997)

- Observation of **three** interband transitions (0-0, 1-1, and 2-2) in absorption spectrum

absorption spectrum
= set of discrete lines ??

- Large spectral width of the lines

$$\Delta E \sim 50 \text{ meV}$$

- Coupling to radiation leads to a **natural linewidth** of

$$\Gamma \sim 1 \mu\text{eV}$$

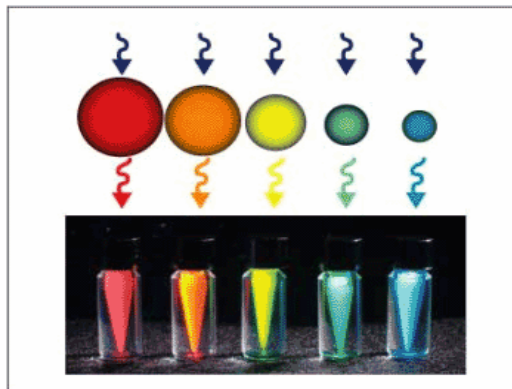


size fluctuations



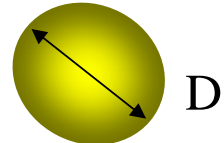
Inhomogeneous broadening

- Optical transition energy

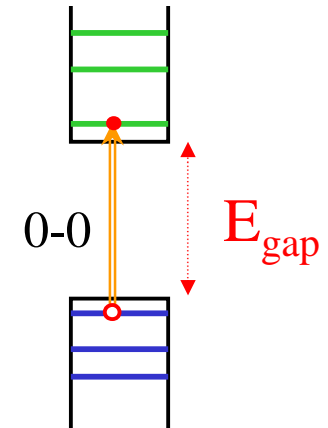


$$E_{n-n} \sim E_{\text{gap}} + E_{\text{confinement}}(n,n)$$

quantum
dot



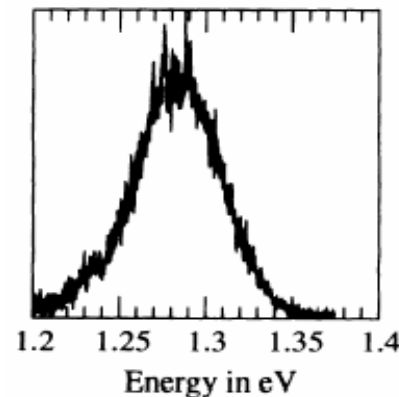
scales like $1/D^2$



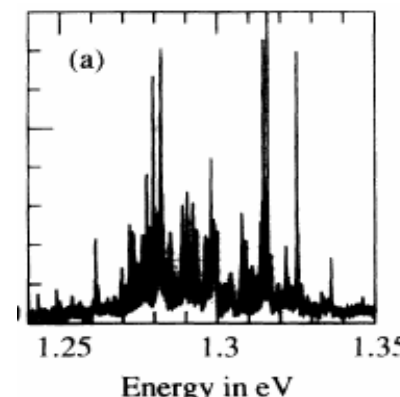
size fluctuations \rightarrow inhomogeneous broadening

- From ensemble measurements to single QD spectroscopy

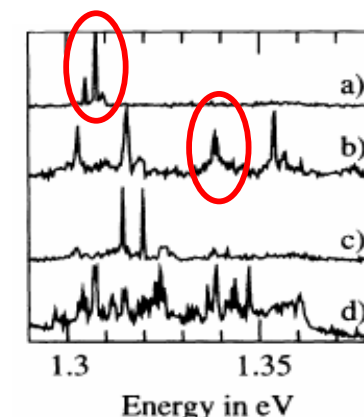
Marzin, PRL 73, 716 (1994)



1000 QDs



10-100 QDs



isolated QDs



Single QD spectroscopy

- Near-field optical spectroscopy

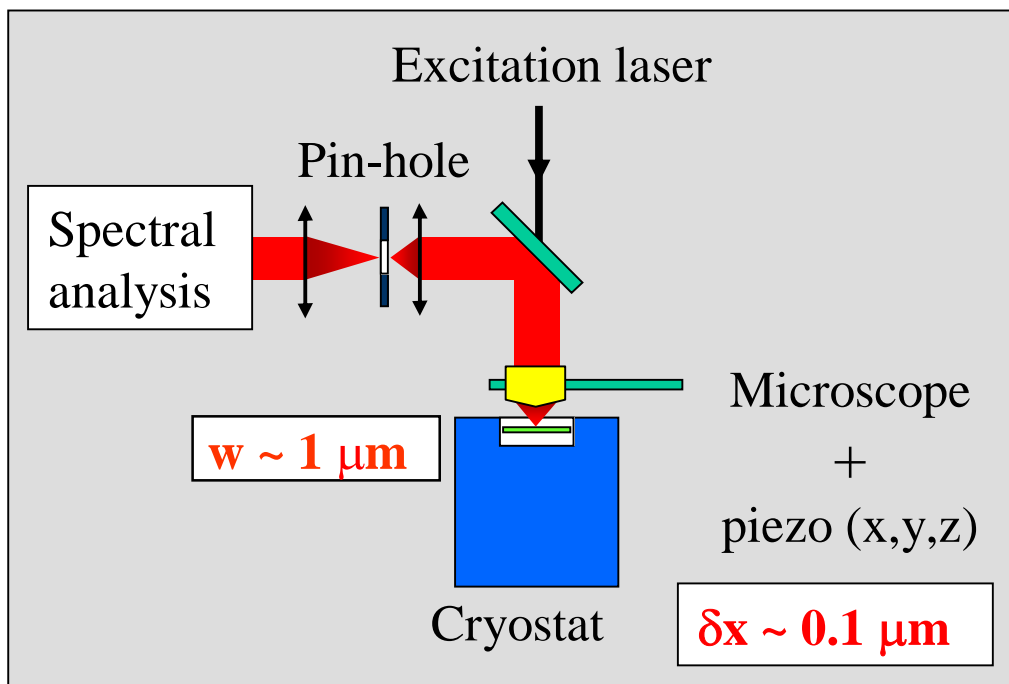
(see [previous lectures](#))

- Far-field optical spectroscopy

Microscope in confocal geometry

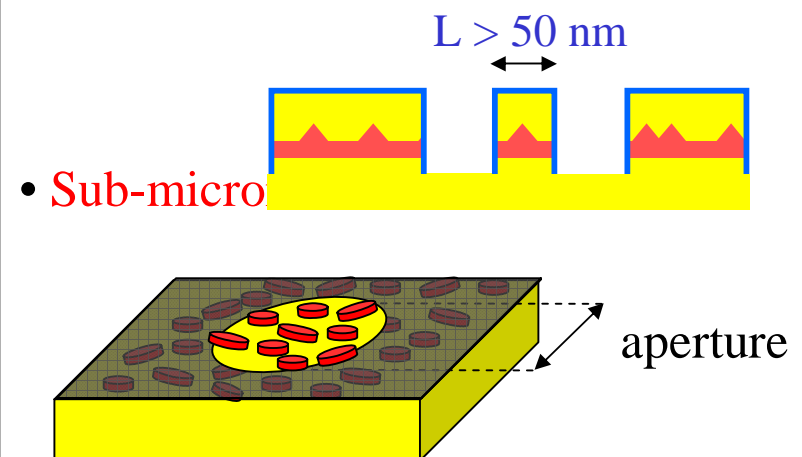


Sample preparation



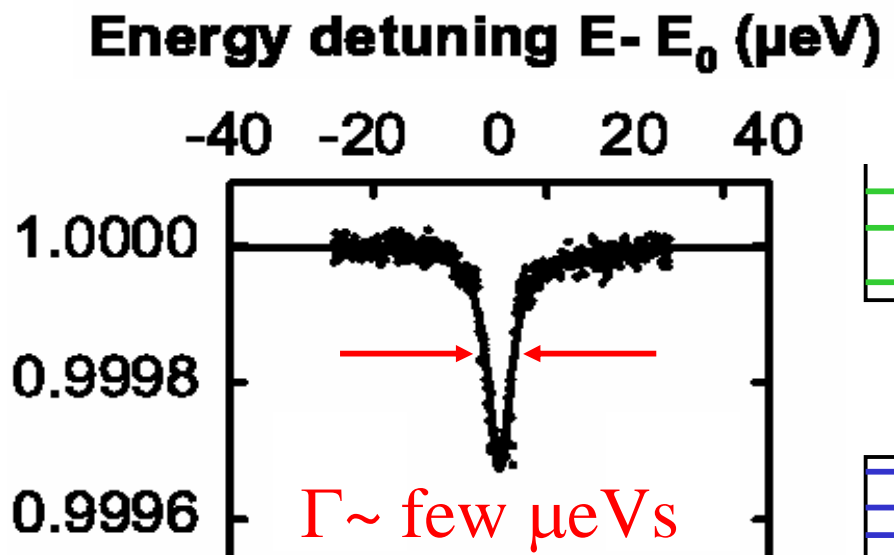
- Dilute QD arrays
 - dispersed solutions of colloidal QDs
 - specific epitaxial growth modes

- Mesa structures



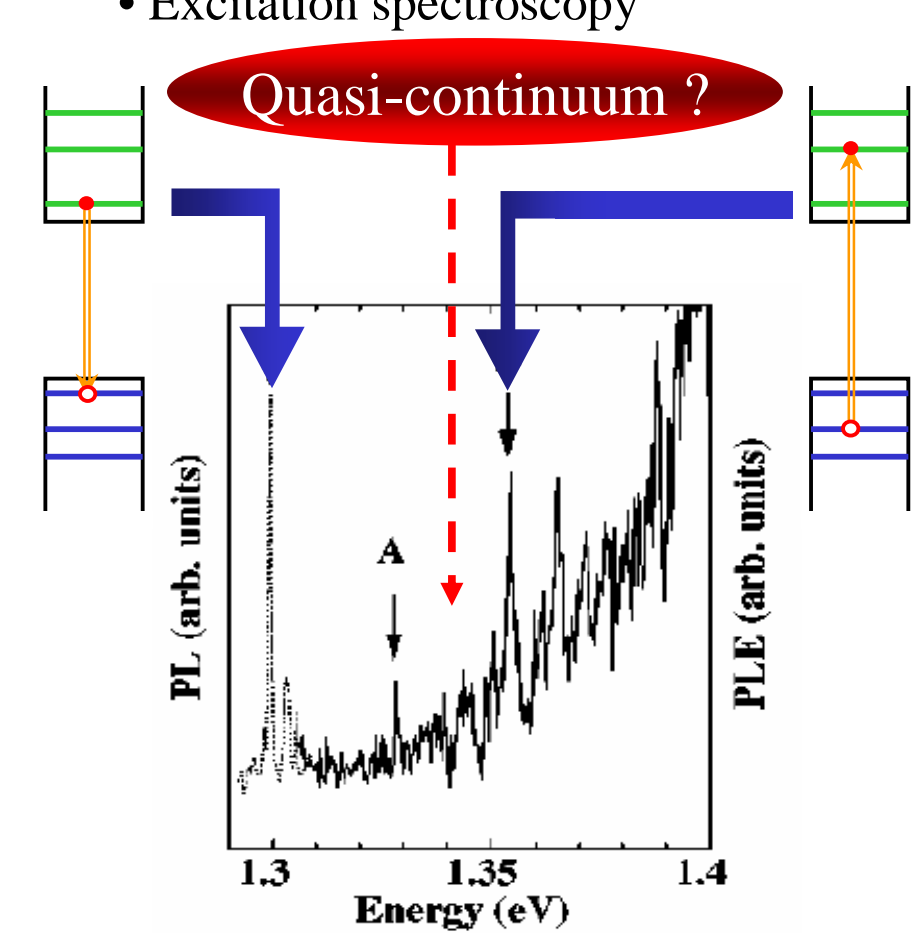
Absorption of a single QD

- Absorption spectroscopy



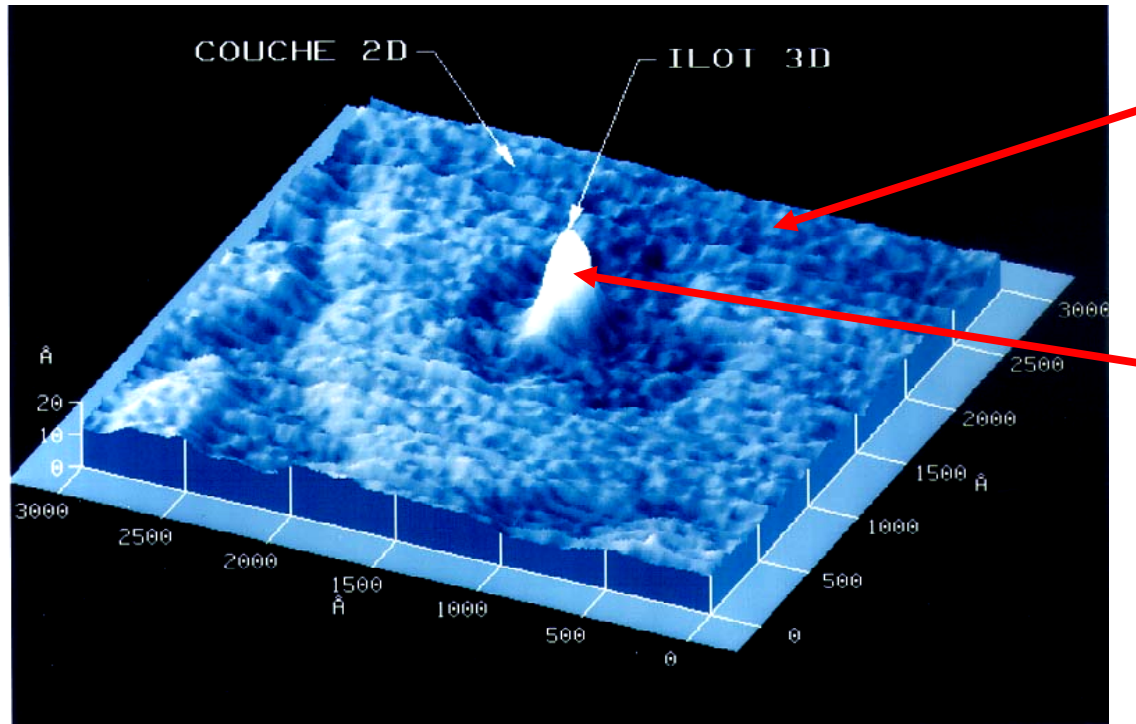
- Fundamental transition = sharp line
- Homogeneous linewidth \sim natural linewidth

- Excitation spectroscopy



InAs/GaAs self-assembled QD

- Morphology of an epitaxially grown QD



J. M. Gérard *et al.*, J. Cryst. Growth **150**, 351 (1995)

InAs **wetting layer**
• thickness ~ 1 nm
(1.7 ML)

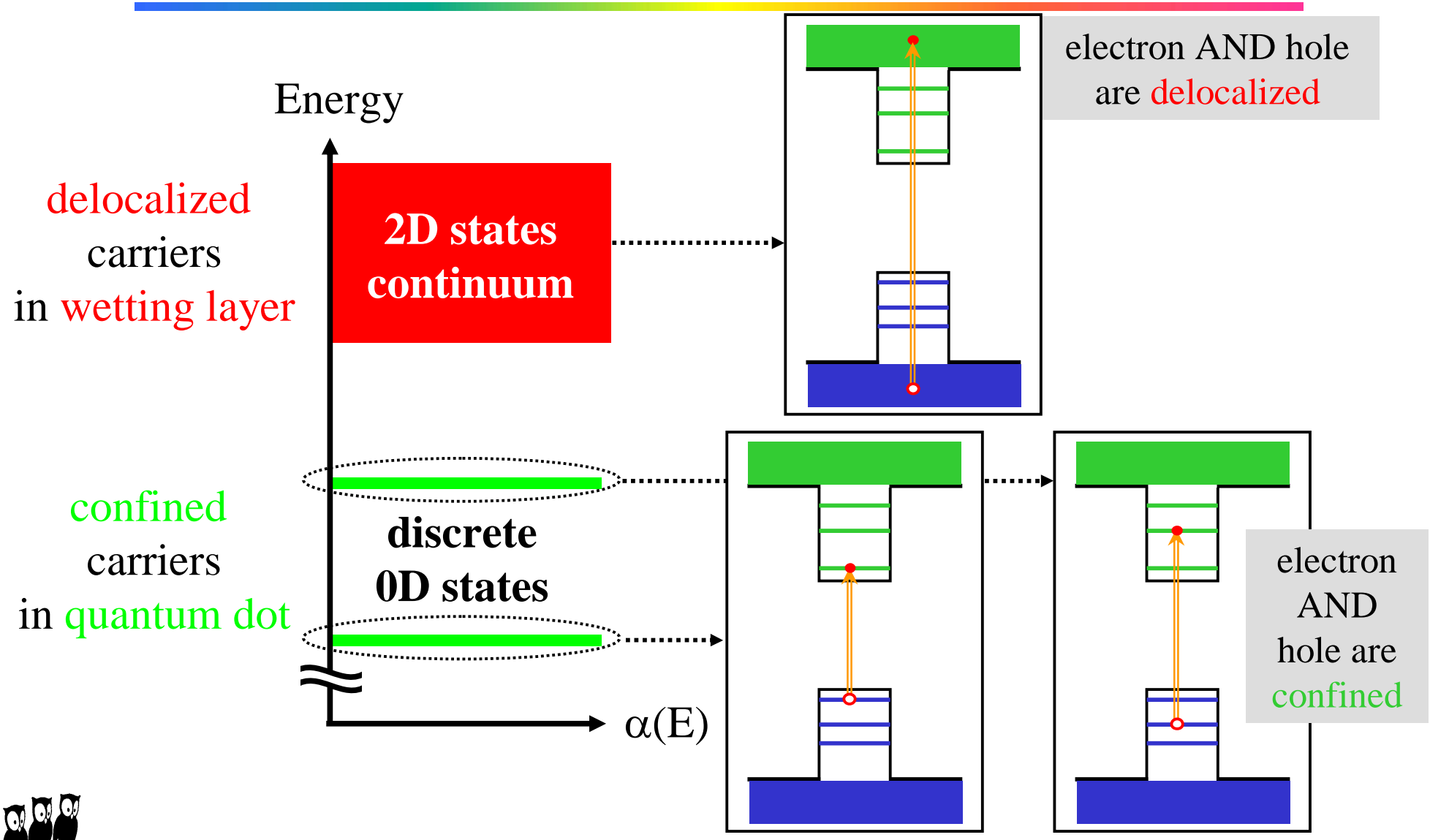
InAs **quantum dot**
• diameter ~ 20 nm
• height ~ 3 nm



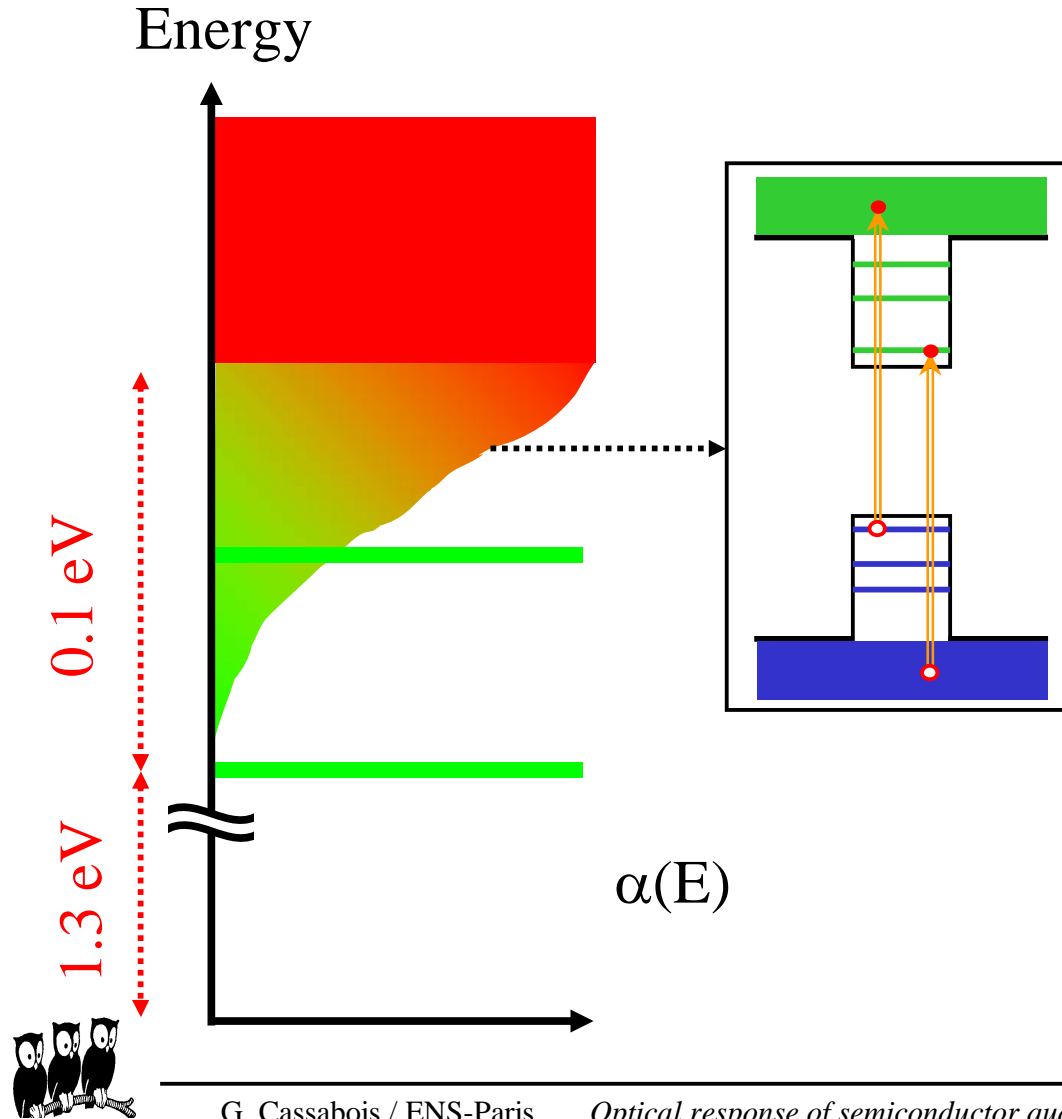
3D confinement of
electrons and holes



2D versus 0D electronic states



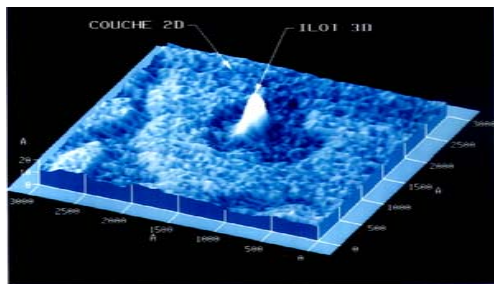
2D-0D interband transitions



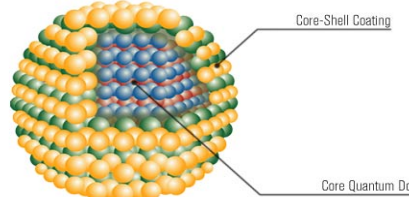
- Interband transitions involve (electron-hole) pairs
 - one shall not miss the cases where
 - hole confined
 - electron delocalized
 - and
 - hole delocalized
 - electron confined
 - Weak transition $|\langle \phi_{2D} | \phi_{0D} \rangle| \ll 1$
 - But one carrier belongs to a quasi-continuum of states
- density of crossed states $\rho_{2D/0D}(E)$

QD = system with discrete lines ?

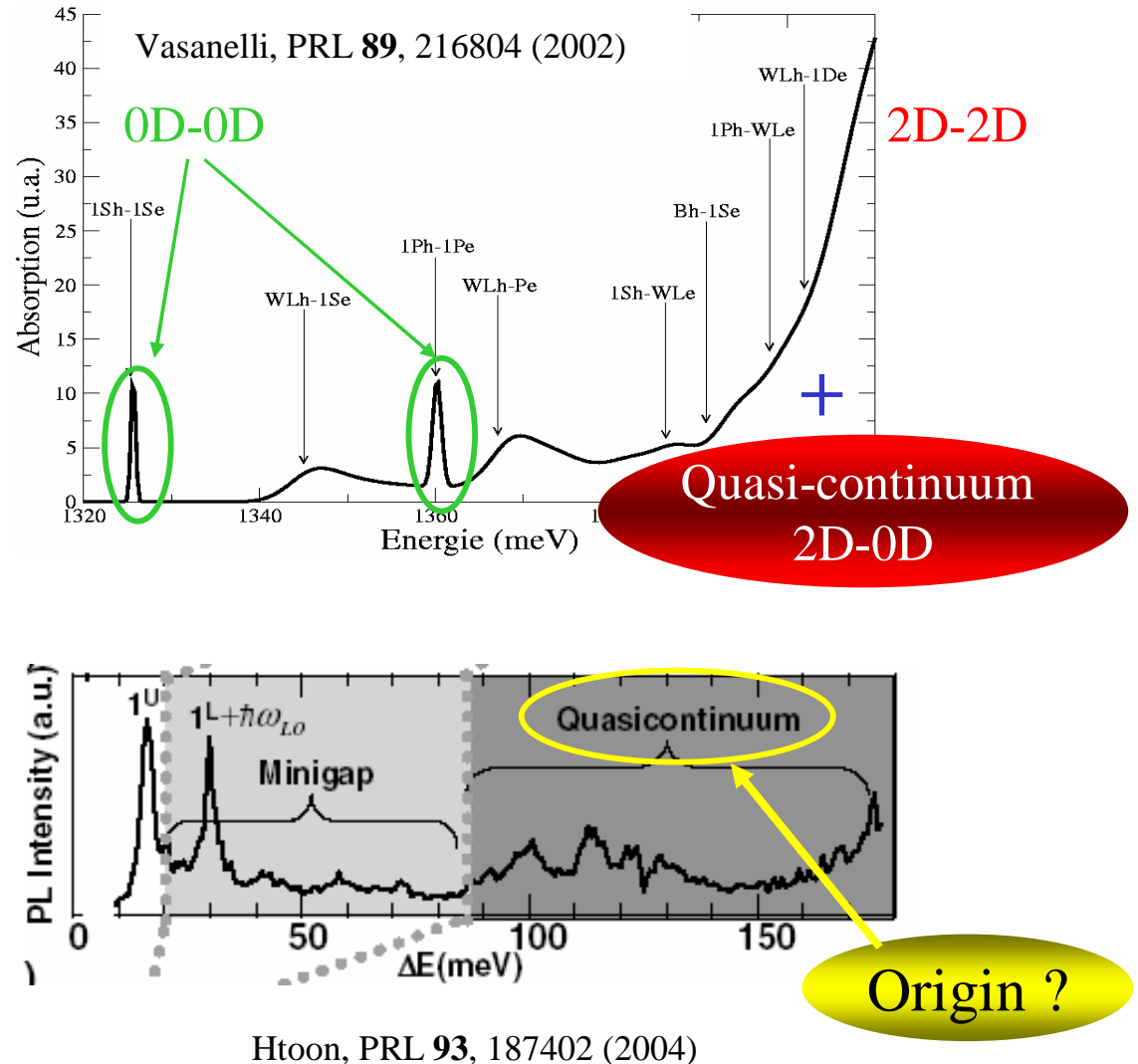
- Epitaxially grown QD



- Colloidal QD

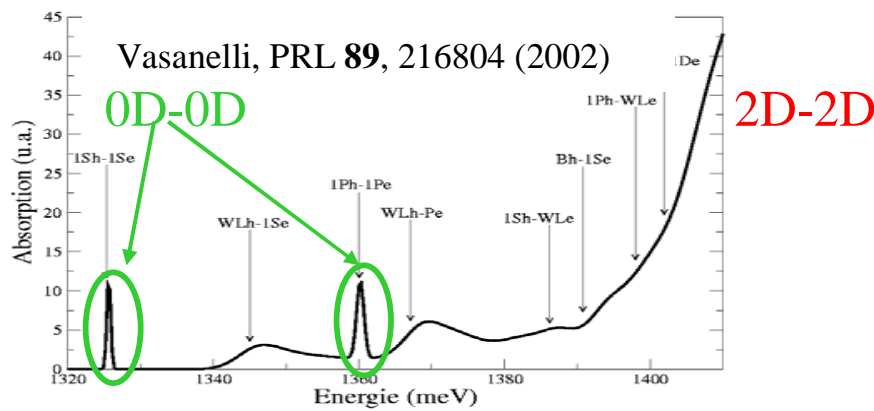
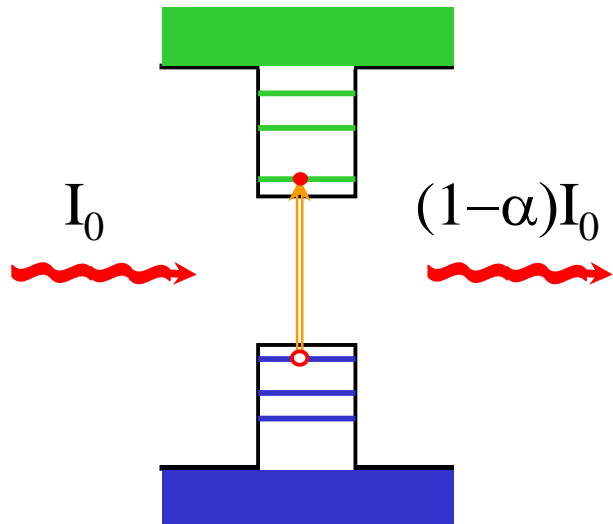


no wetting layer
but an insulating matrix
no 2D-0D quasi-continuum

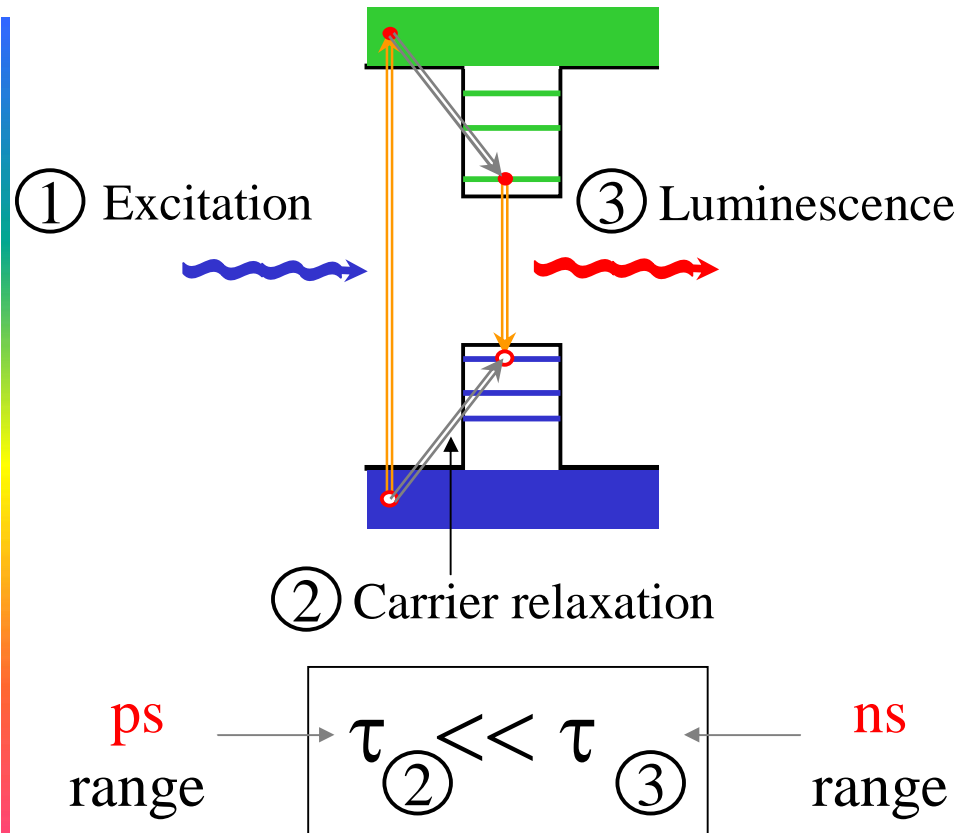


From absorption to emission

- Absorption



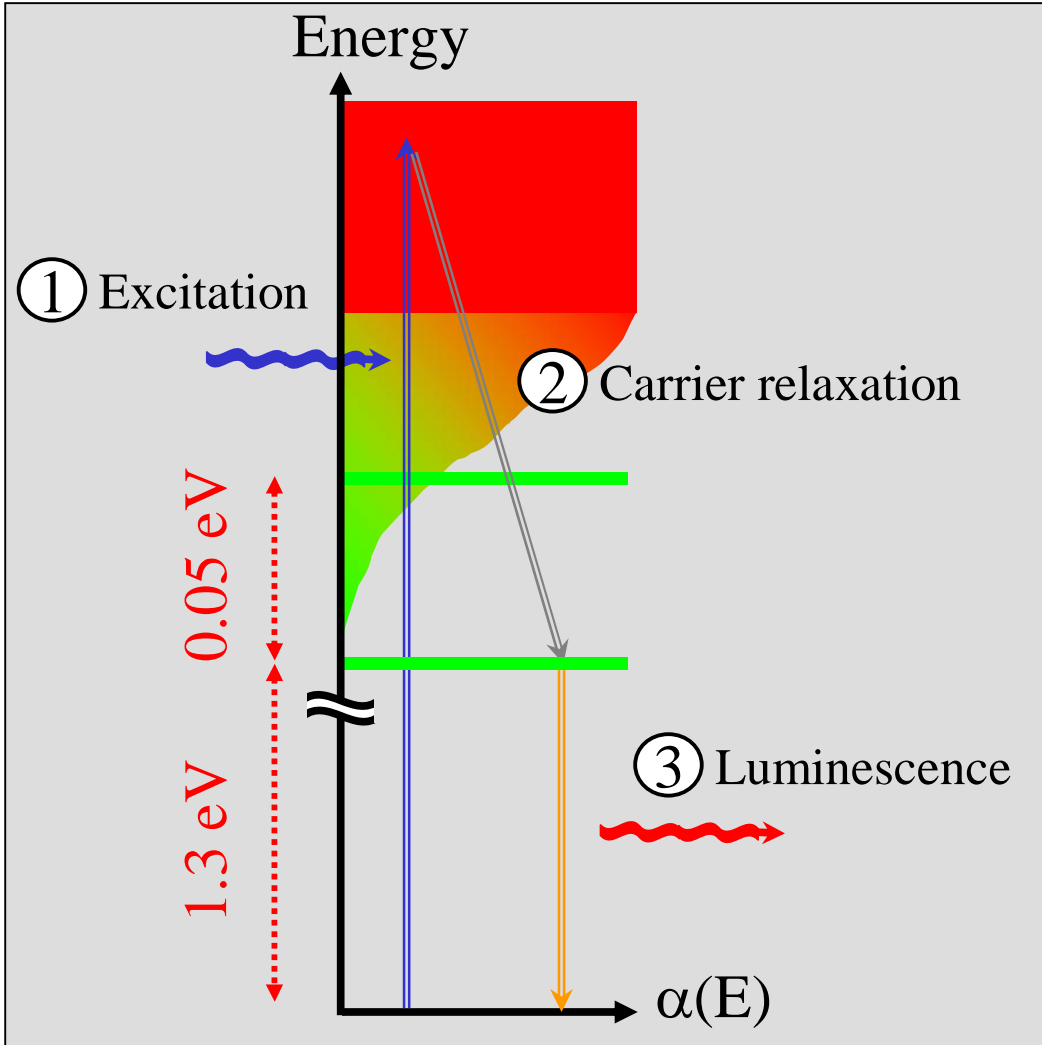
- Emission



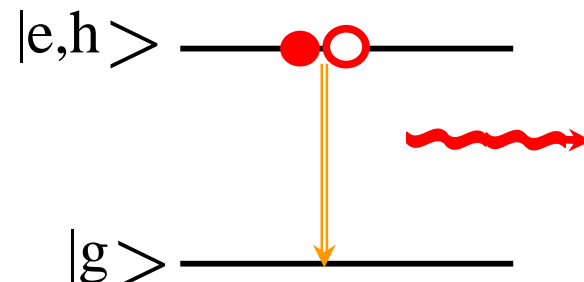
Emission comes
only from the lowest transition



Two-level system approximation



- QD = complex system in solid state physics
BUT
the efficient carrier relaxation
shortcuts the **dimensionality transition**
in the QD absorption spectrum
- **Two-level system** = first-order
approximation for the description of
the QD optical response in **emission**



Fundamental transition fine structure

- Fundamental **interband** transition corresponds to (e,h) **pair state** with a **heavy**-like hole

$$\begin{aligned} |electron\rangle &= |J = 1/2, J_z = \pm 1/2, \dots\rangle \\ |heavy\ hole\rangle &= |J = 3/2, J_z = \pm 3/2, \dots\rangle \end{aligned}$$

- Four-fold **degeneracy**

$$\begin{aligned} |e, h\rangle &= |J = 2, J_z = +1, \dots\rangle \text{ emits } \sigma_+ \text{ light} \\ &= |J = 2, J_z = -1, \dots\rangle \text{ emits } \sigma_- \text{ light} \\ &= |J = 2, J_z = +2, \dots\rangle \text{ no emission} \\ &= |J = 2, J_z = -2, \dots\rangle \text{ no emission} \end{aligned} \quad \left. \begin{array}{l} \text{bright states} \\ \text{dark states} \end{array} \right\}$$

- **Coulomb** interaction between pair states

$$\langle \psi_{c'}(1), \psi_{v'}(2) | V_c | \psi_c(1), \psi_v(2) \rangle \quad \text{direct interaction term}$$

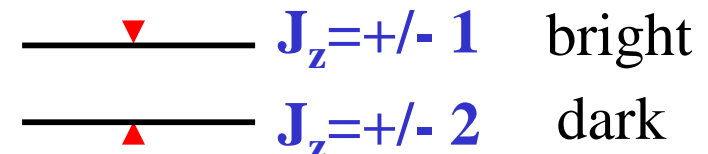
$$\langle \psi_{c'}(1), \psi_{v'}(2) | V_c | \psi_v(1), \psi_c(2) \rangle \quad \text{indirect or exchange interaction term}$$



Dark and bright states

- Short range part of exchange interaction lifts degeneracy of bright and dark states

0.5 meV (InAs) – 4 meV (CdSe)



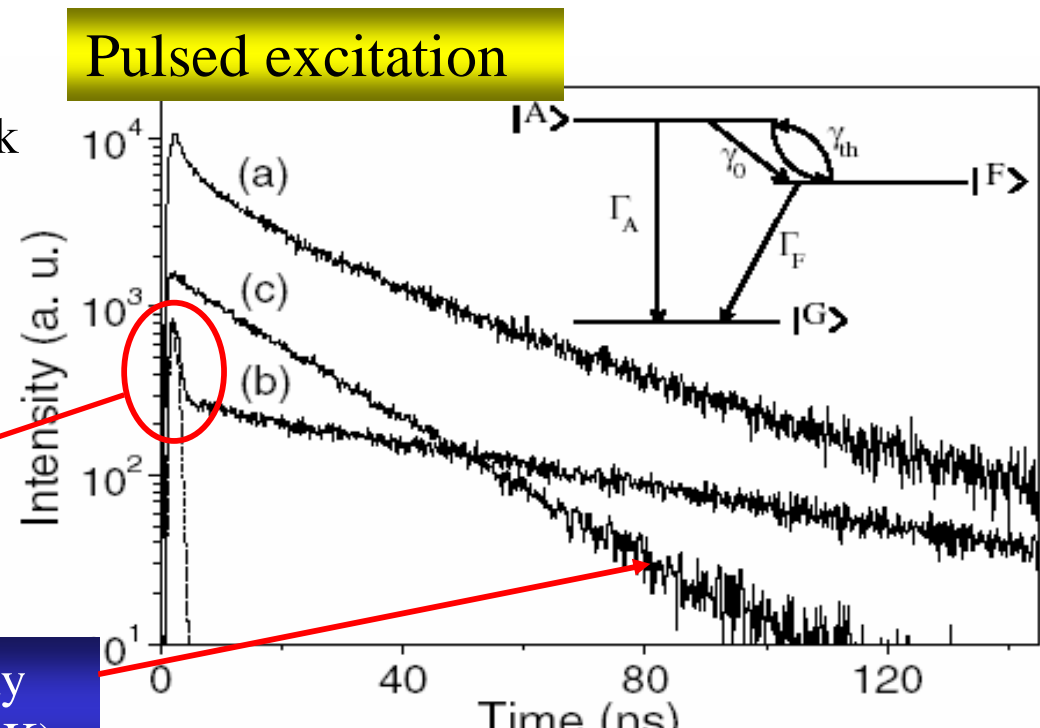
- No luminescence from dark states

BUT

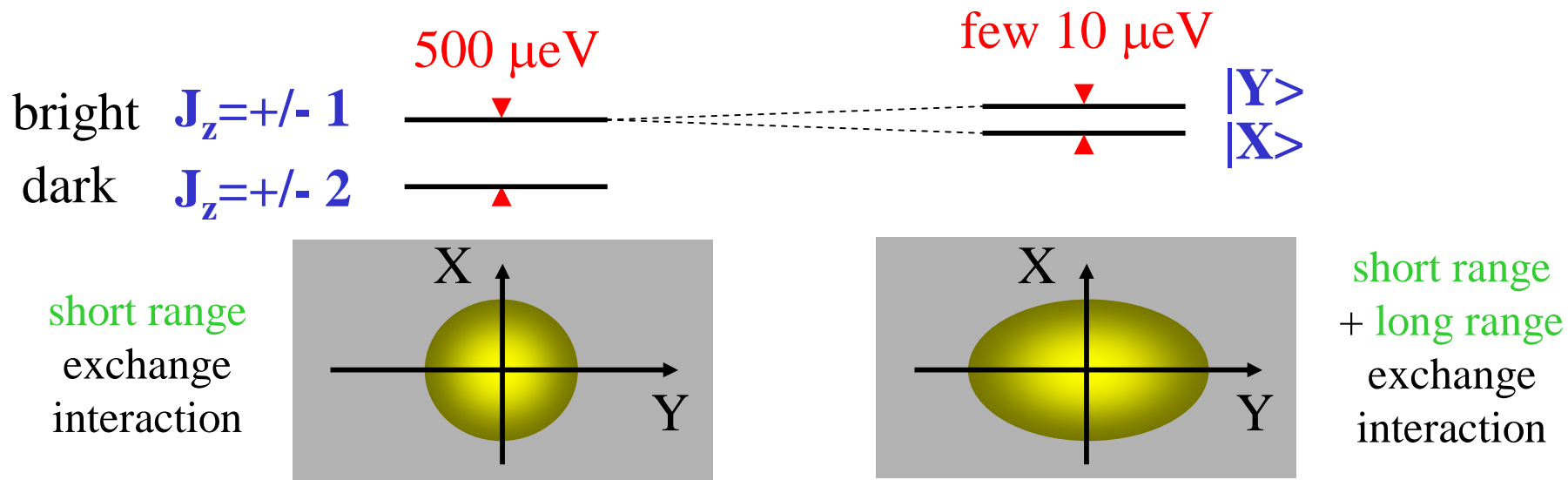
interplay between the bright and dark states during population relaxation dynamics

Bi-exponential decay at low temperature (16K)

Mono-exponential decay at high temperature (140K)



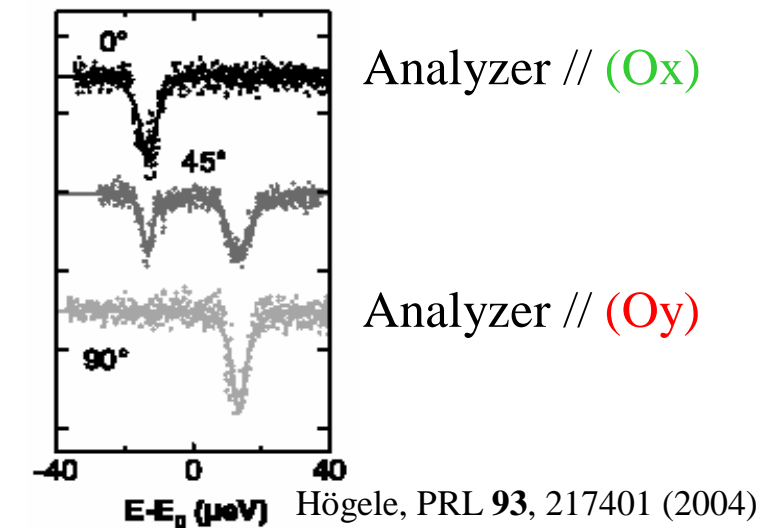
Rotational symmetry breaking



- In a QD of **broken symmetry** the new bright states emit **linearly polarized light**

$$|X\rangle = \frac{|+1\rangle + |-1\rangle}{\sqrt{2}}$$

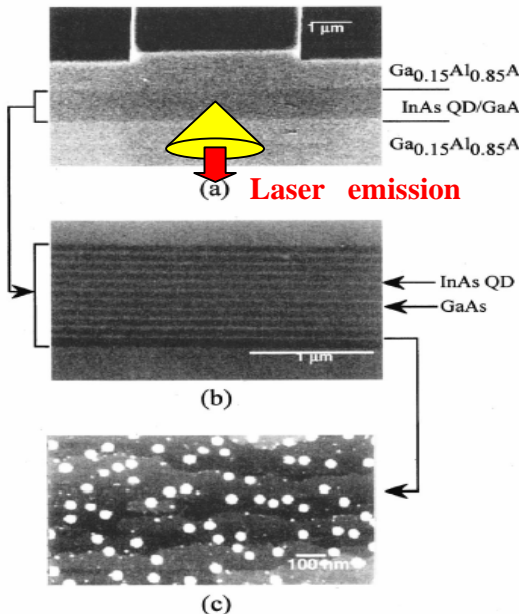
$$|Y\rangle = \frac{|+1\rangle - |-1\rangle}{i\sqrt{2}}$$



From fundamental optical properties to optical applications



QD laser



Nakamura
J. Appl. Phys. **94**, 1184 (2003)

QD laser

Opto-electronics



- Gain and threshold current density of ideal QD laser (no inhomogeneous broadening)

Arakawa and Sakaki APL **40**, 939 (1982)

- higher maximum gain due to narrow gain spectrum (0D density of states)
- no temperature dependence of threshold current

- size fluctuations in real QD laser > inhomogenous broadening to be reduced
- existence of intrinsic limit = homogeneous linewidth due to phonon coupling ($\Gamma \sim 10$ meV at 300K)
- no quenching of carrier escape

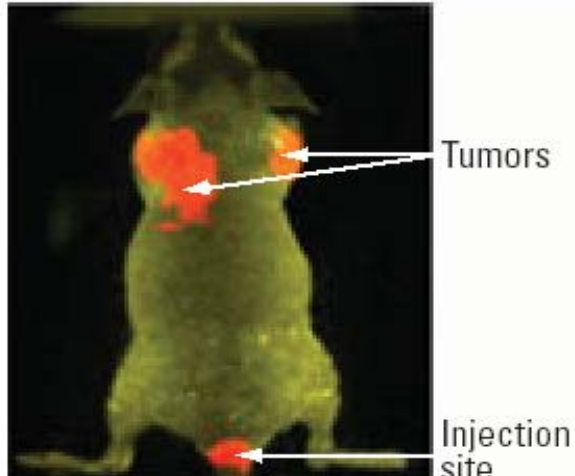
QW versus QD lasers = ?

Biological sensors

Bio-physics

Biological sensors

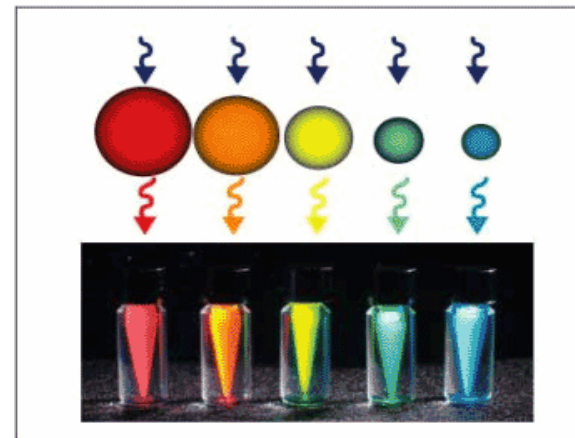
In vivo imaging of cancer cells in a living mouse



Gao, Nature Biot. 22, 969 (2004)

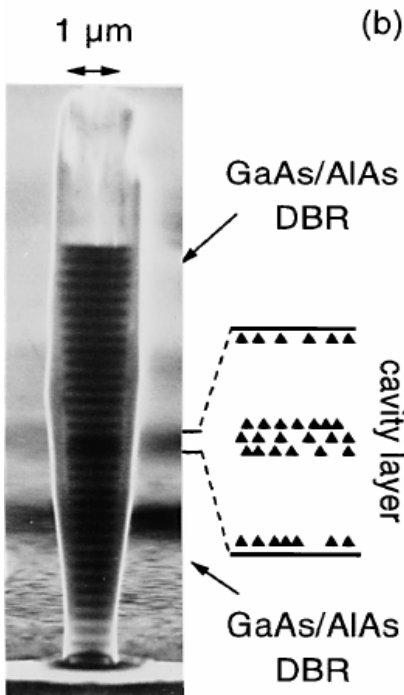


- colloidal QDs
- broadly tunable in the visible spectrum by size variation



- high quantum efficiency
 - bio-conjugating colloidal QDs (cell labeling, cell tracking, *in vivo* imaging, DNA detection, multiplexed beads...)
- (see Alivisatos, Nature Biot. 22, 47 (2004)
and [previous lectures](#))

Single photon source



Gérard, PRL **81**, 1110 (1998)

- single QD generates **single photon state**
- non-classical source of radiation : **sub-Poissonian** statistics
- **quantum optics** in solid state
- **quantum information processing**

Single photon source

Quantum optics



Quantum optics in solid state with a non-classical source of radiation

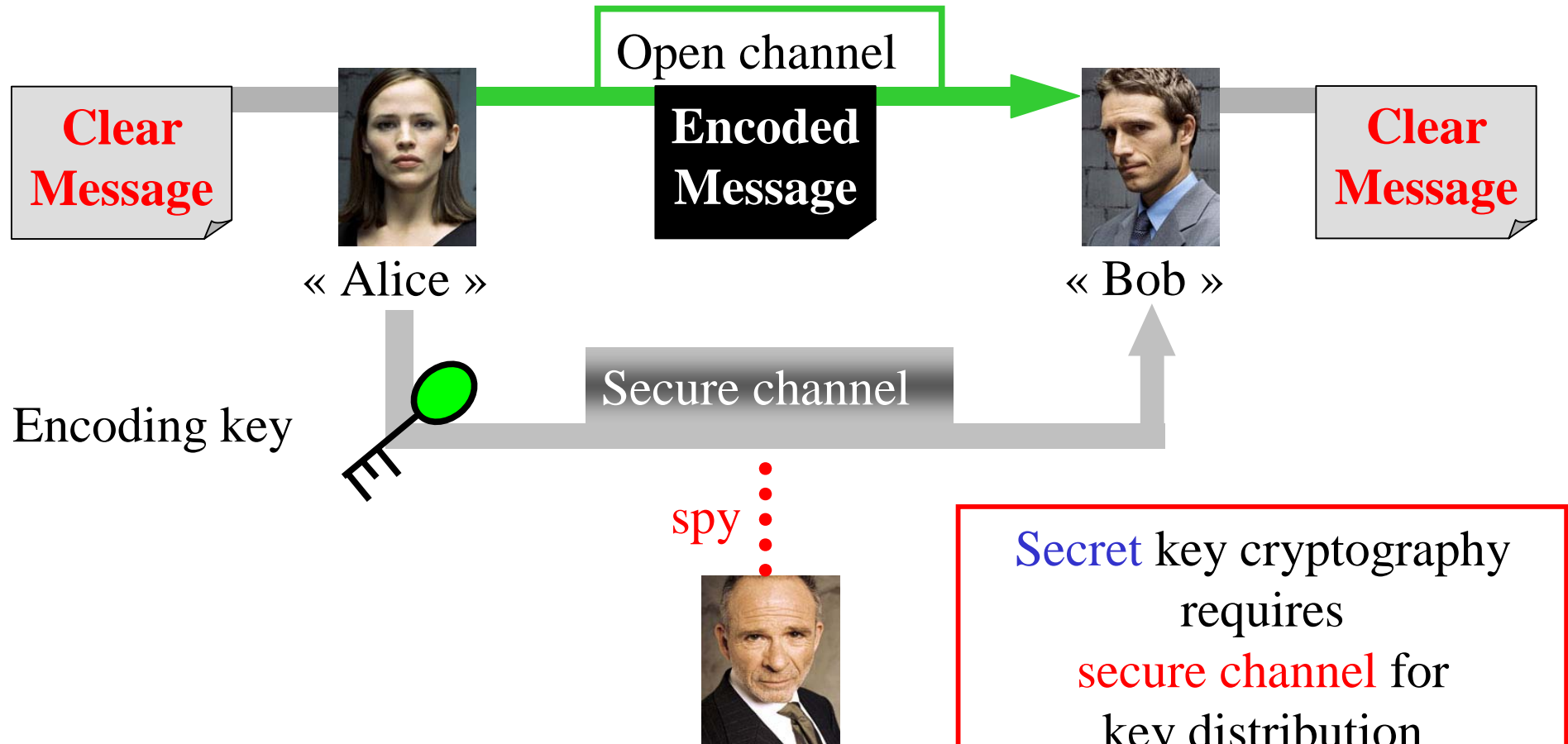
Outline

- quantum cryptography
- single-photon source
- carrier quantum cascade



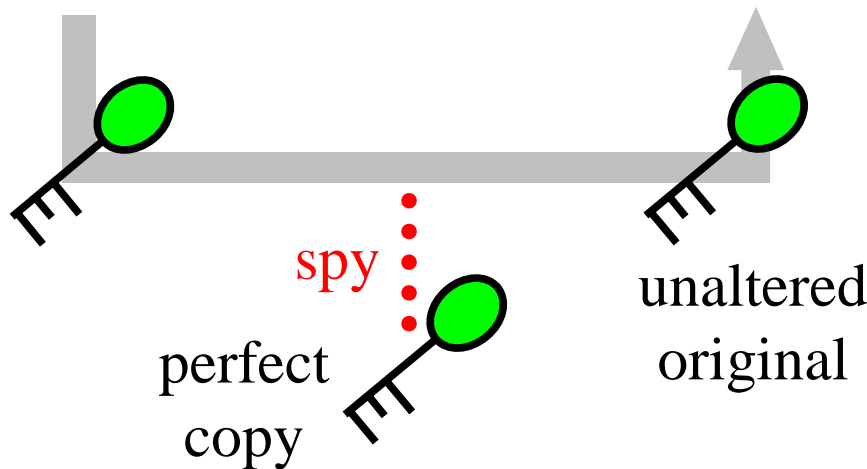
Secret key cryptography

- Goal : transmission of **secret** message



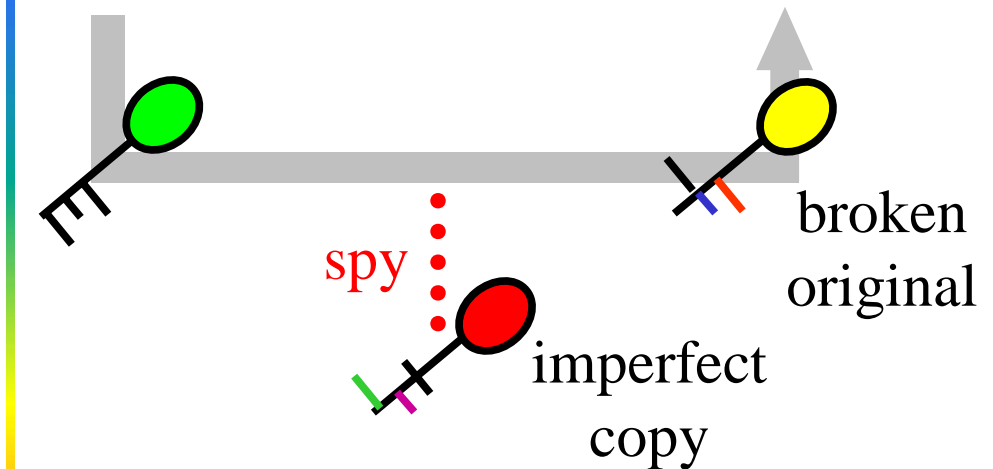
Classical versus quantum information

- Classical information



in principle every classical channel
can be monitored passively

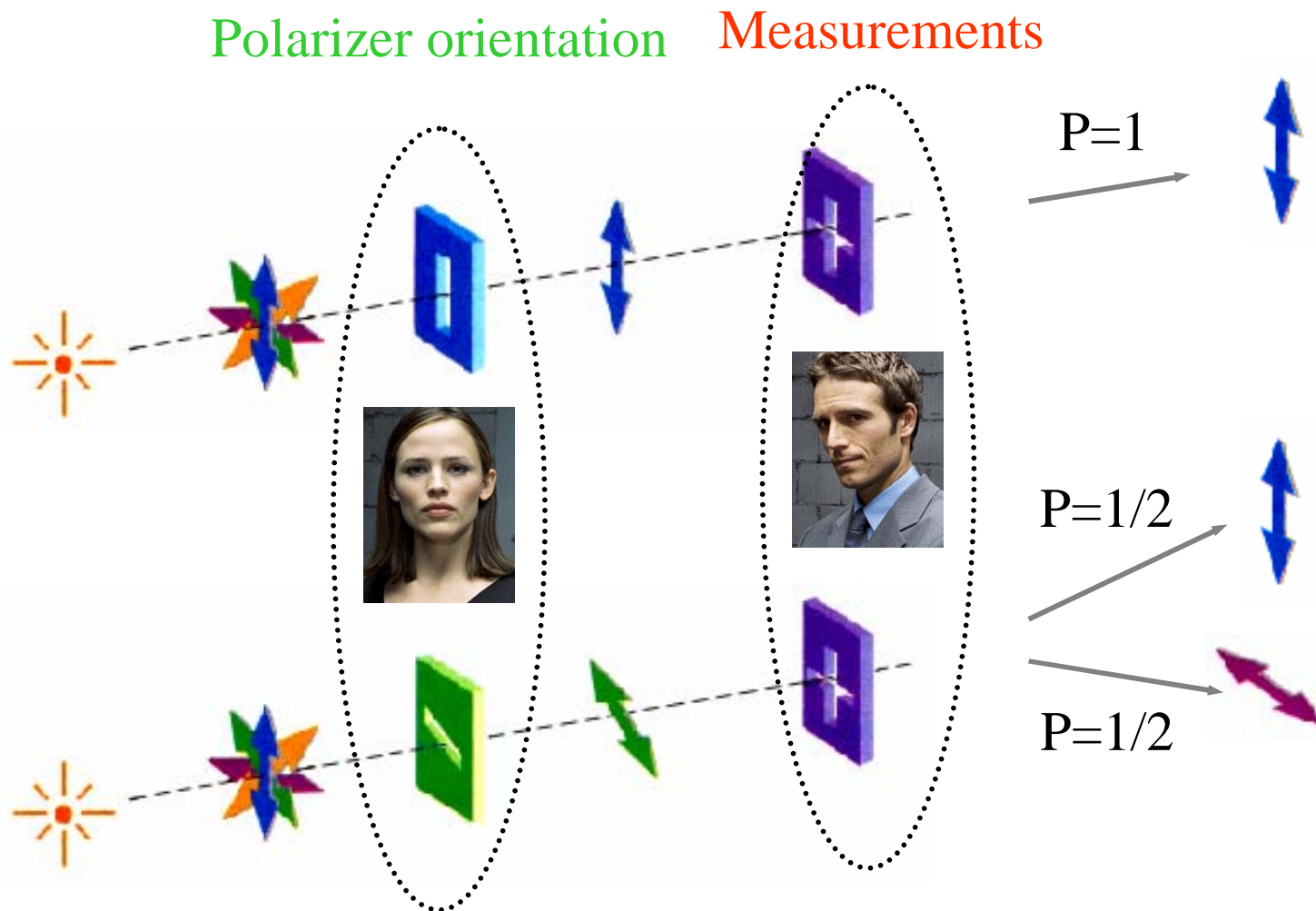
- Quantum information



- quantum cryptography distributes the key by transmitting quantum photon states in an **open channel**
- this **open channel** is **intrinsically secure** because a spy destroys the encoding key



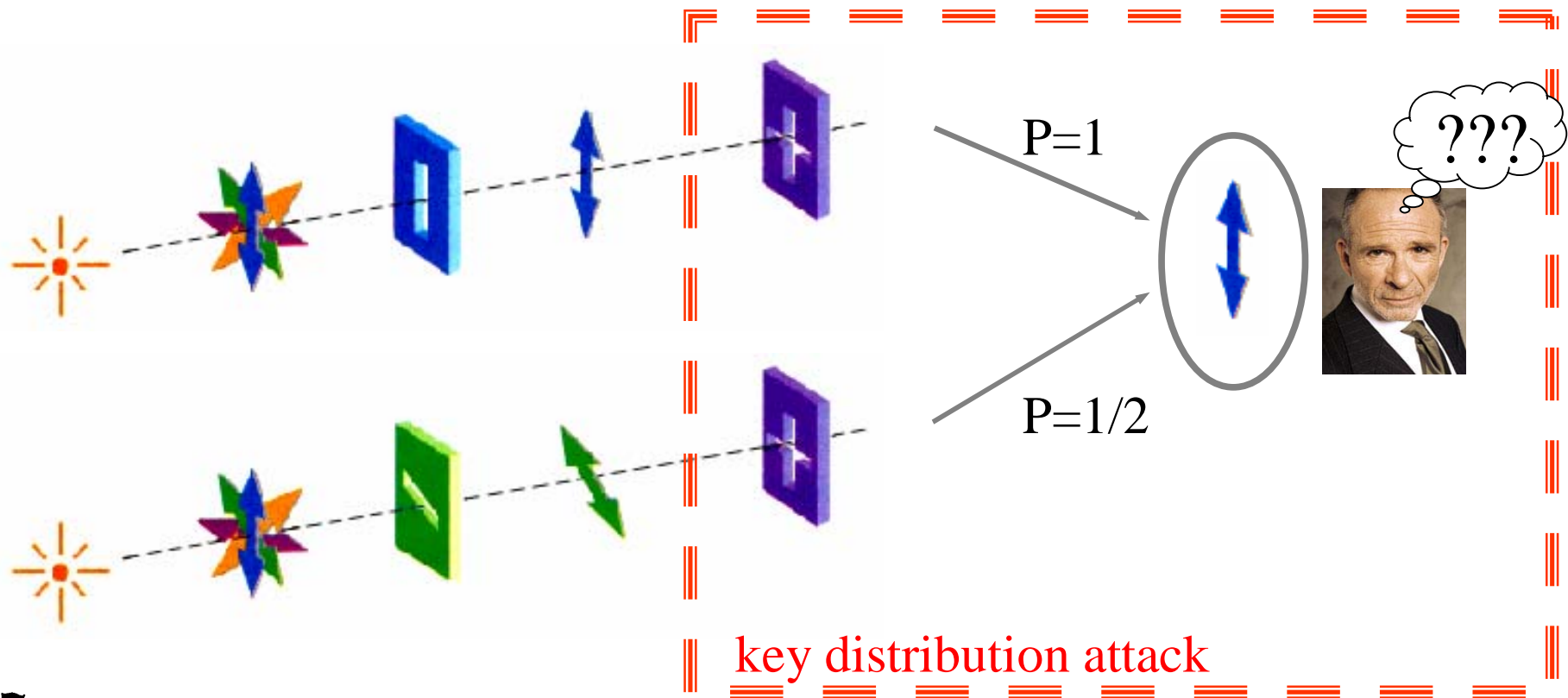
Polarization state of a single photon



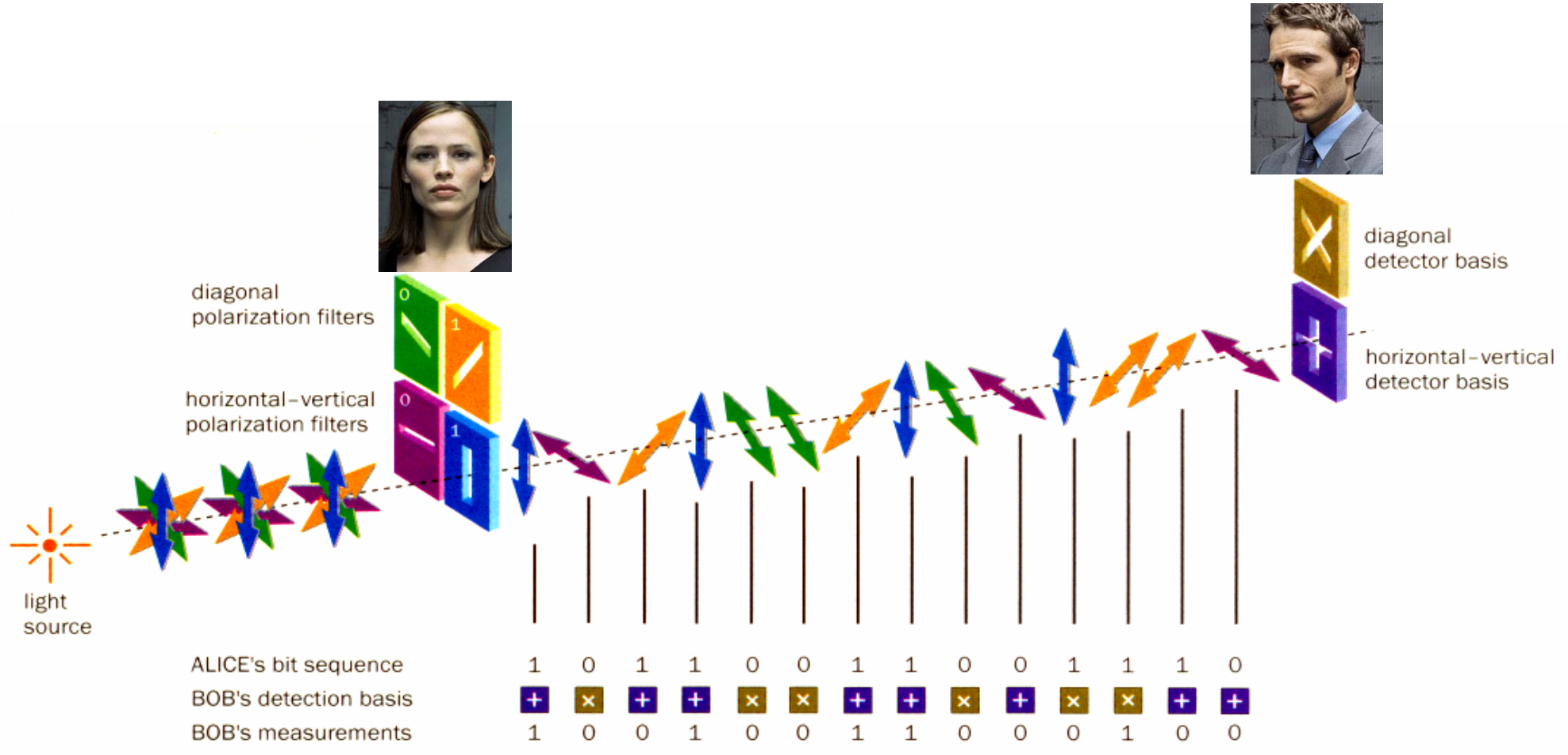
Spy measurements

- Importance of having **two** polarization basis to avoid perfect copy of single photon state

||  the spy will generate **errors** in the key distribution

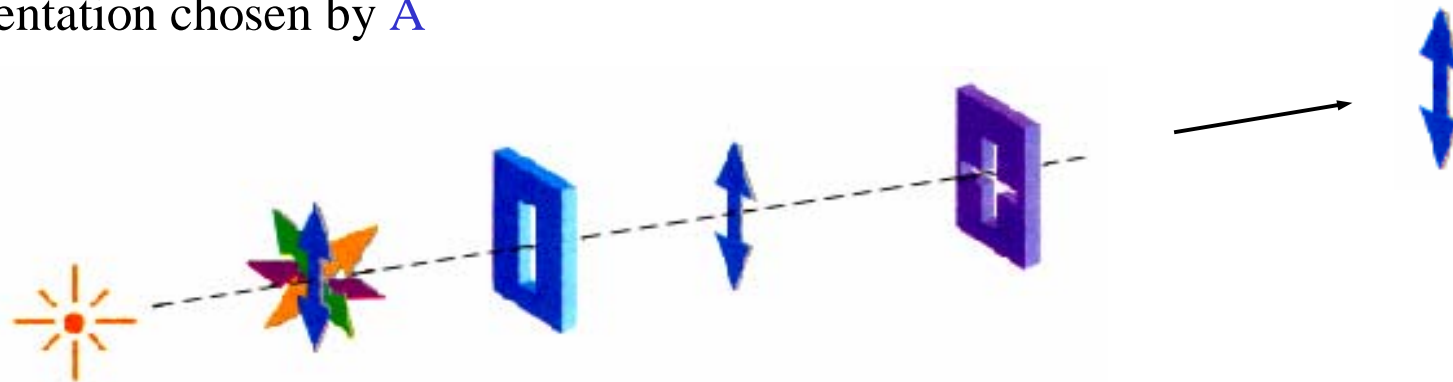


Quantum key distribution



Key distribution analysis

- **B** sends to **A** by open channel his set of detection basis and half of his measurements
- **A** selects the cases where the detection basis corresponds to the polarizer orientation chosen by **A**



in that cases **B** must have found the same result as **A**
if not, this means there is a spy which has generated a single photon with an incorrect polarization orientation !

- among the retained bit sequence, **A** chooses a subset of bits to compose the **encoding key** and sends the location of these bits in the total message to **A** by open channel

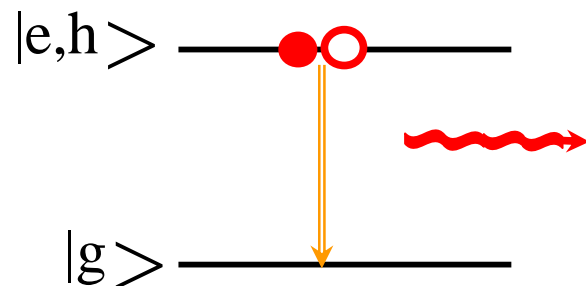


Single QD as single-photon source



Solid-state single-photon source

- single QD



- radiative recombination of **single** (e,h) pair generates single photon
- this picture breaks down for a **QDs ensemble**

- quantum **wire** (1D), quantum **well** (2D)

continuum of electronic states

$E_{|e,h\rangle}$

radiative states

non-radiative states

k_0

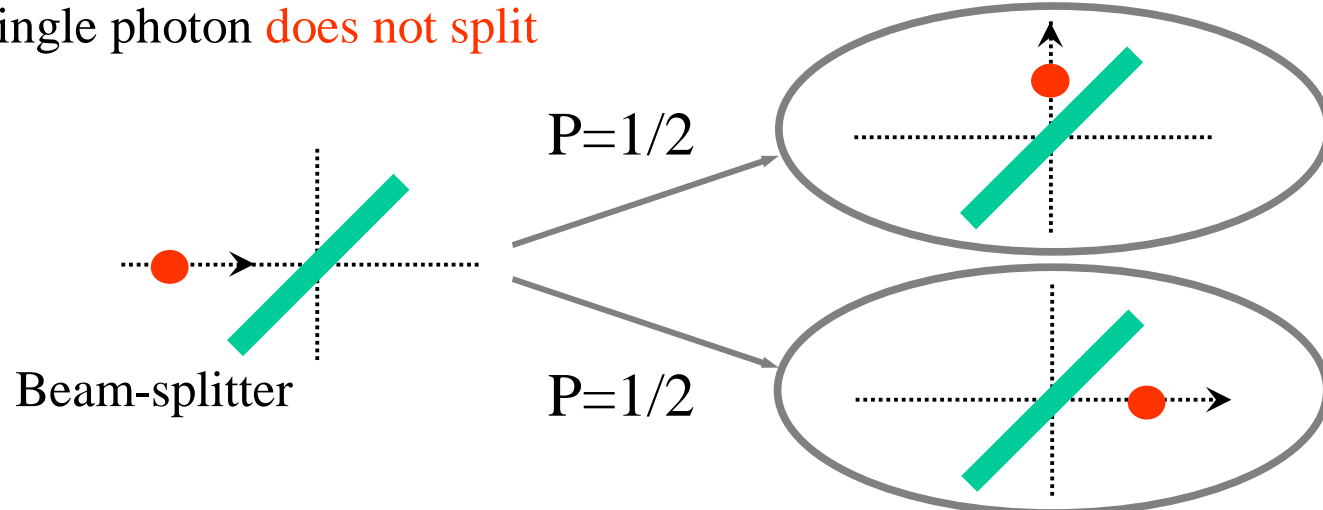
k

translational quantum number

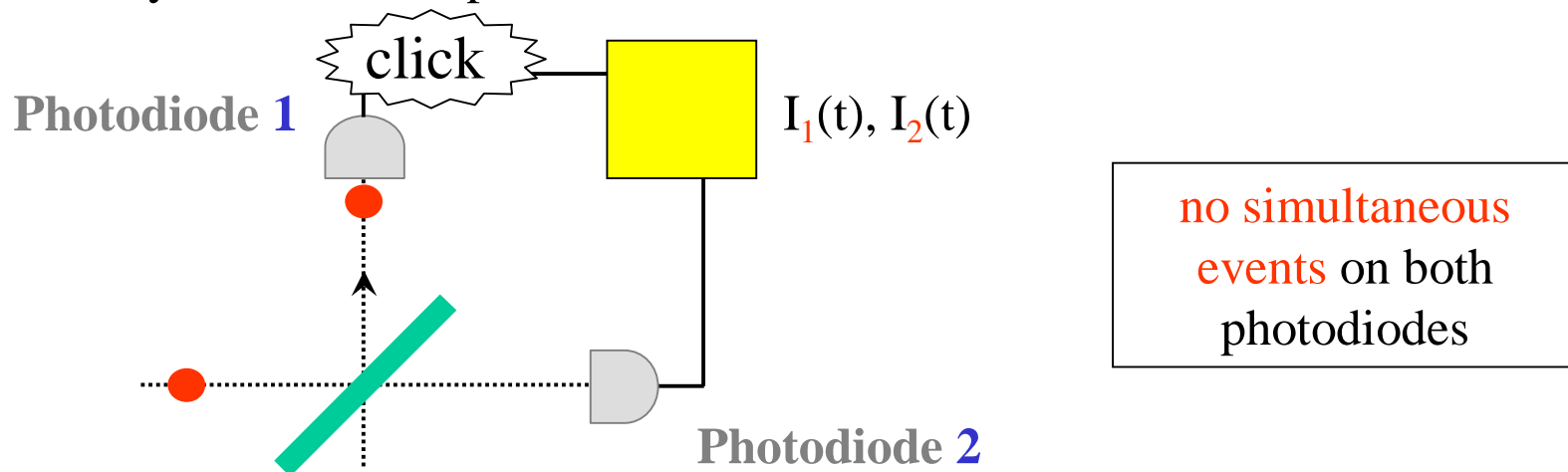


Coincidence detection

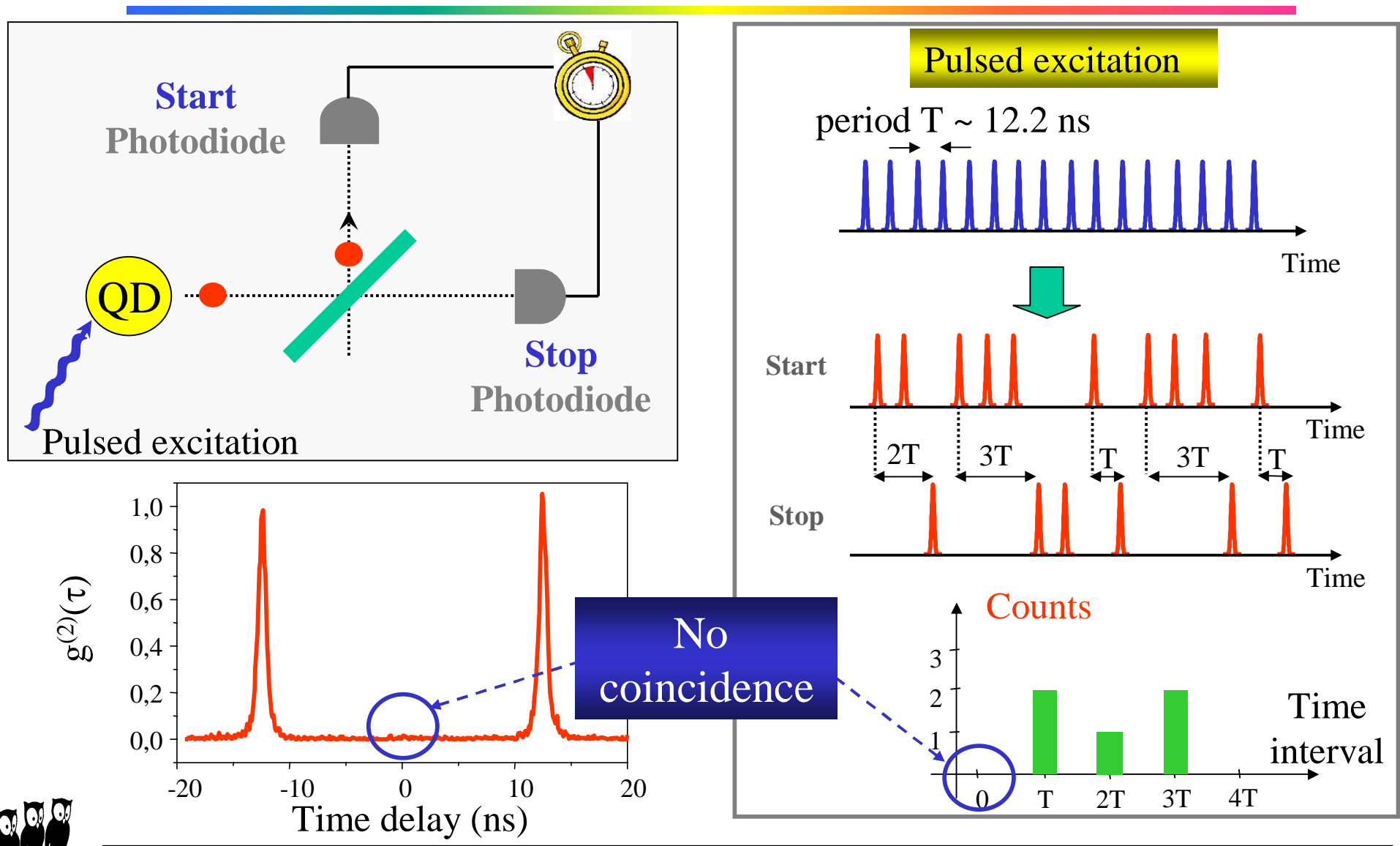
- single photon **does not split**



- intensity **correlation** experiments



Start-stop correlation experiments

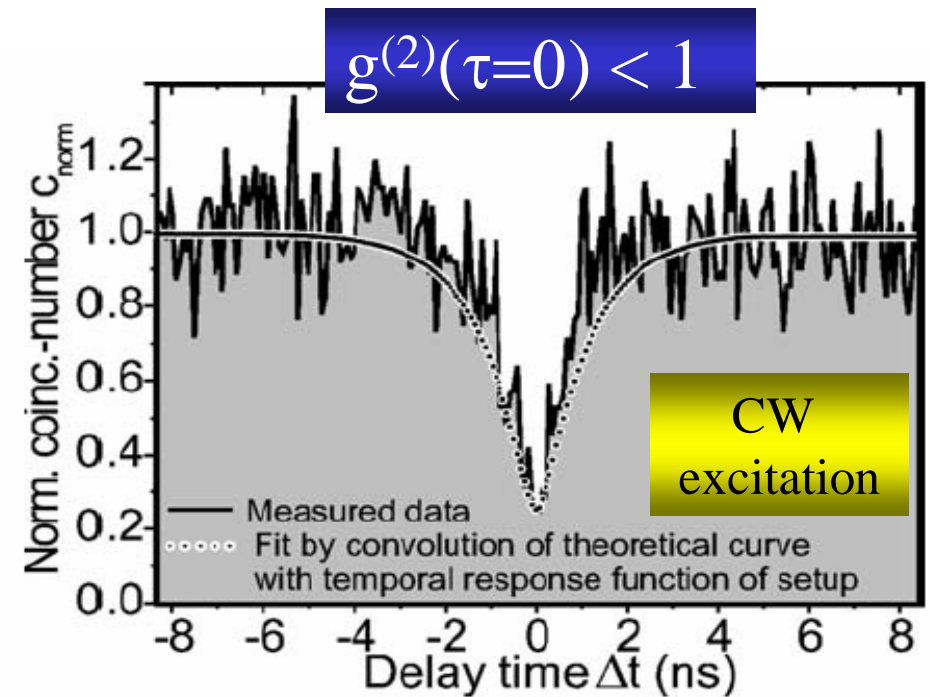
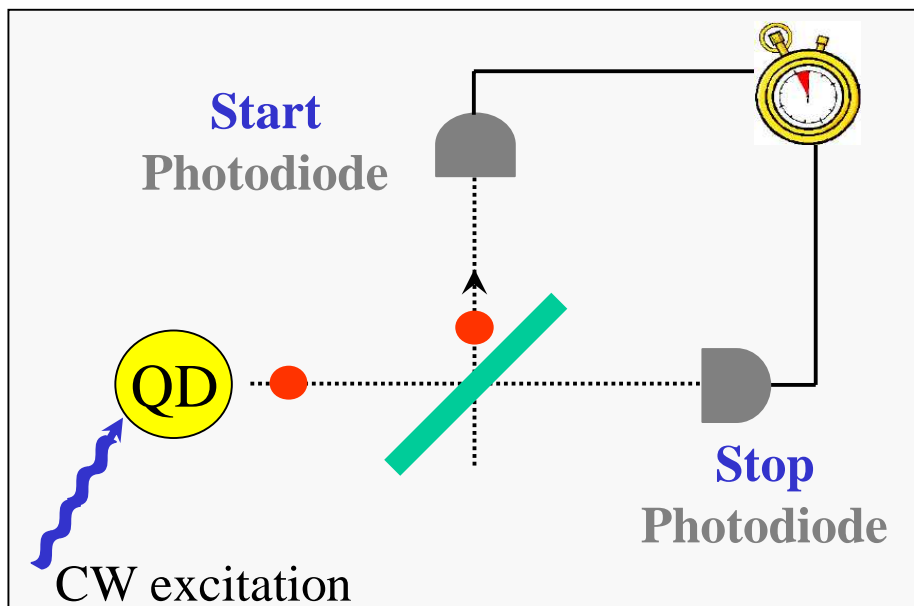


Photon anti-bunching

- normalized intensity correlation function $g^{(2)}(\tau)$

$$g^{(2)}(\tau) = \frac{\langle I_1(t)I_2(t + \tau) \rangle}{\langle I_1(t) \rangle \langle I_2(t) \rangle}$$

- start-stop correlation experiments under continuous-wave excitation

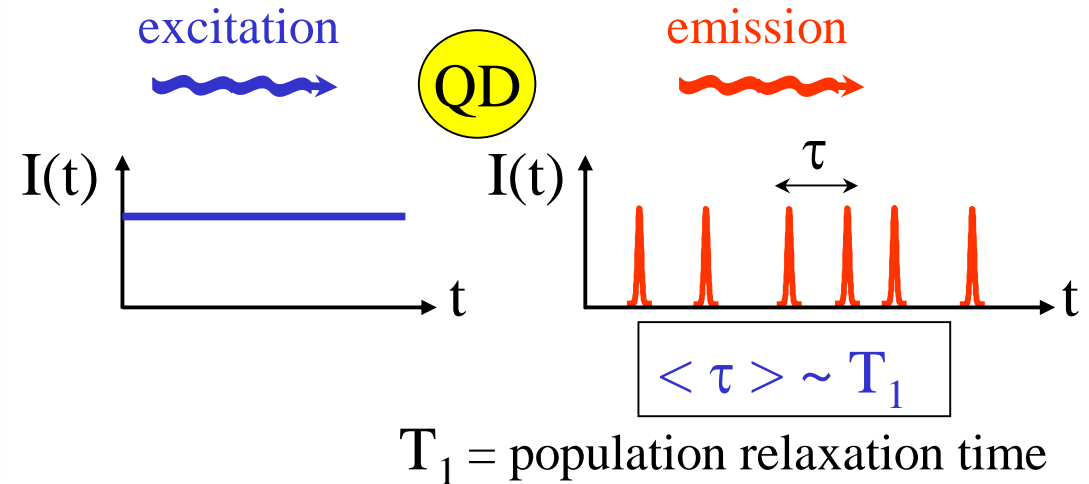
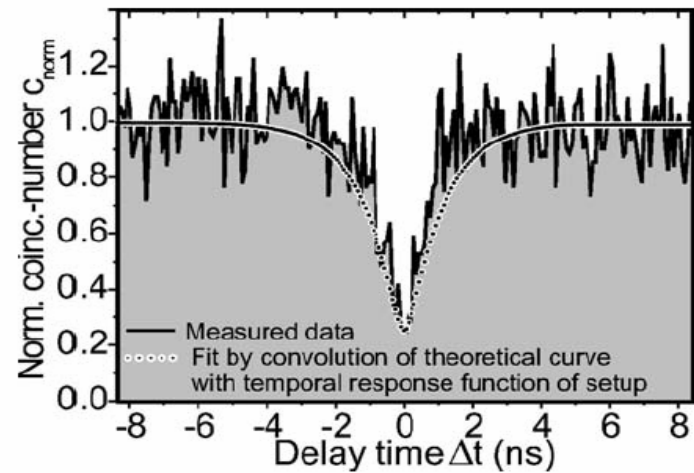


Baier, APL **84**, 648 (2004)

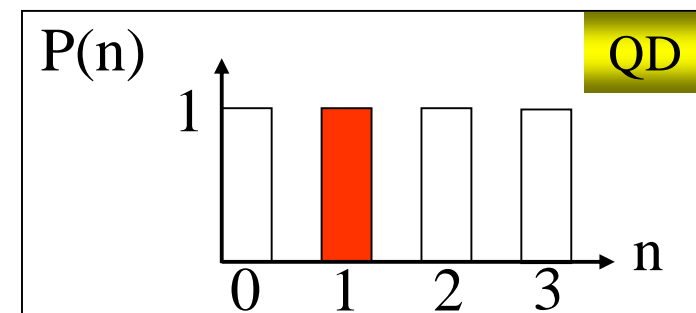
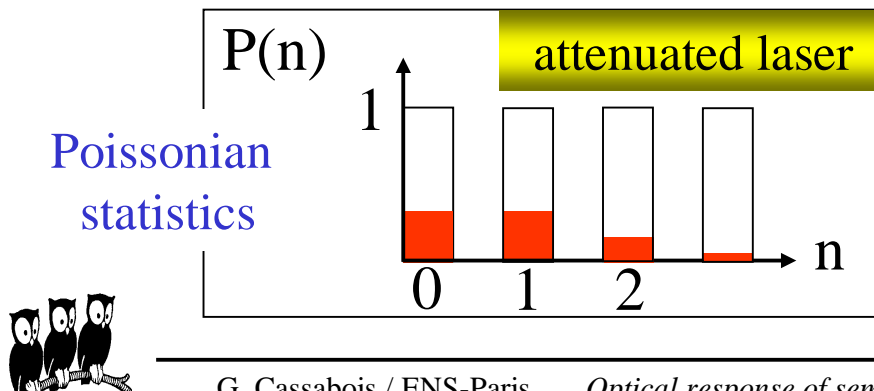


Sub-poissonian statistics

- $g^{(2)}(\tau=0) < 1$ reveals non-classical character of light source
- sub-poissonian photon statistics



- attenuated laser versus single QD when $\langle n \rangle = 1$

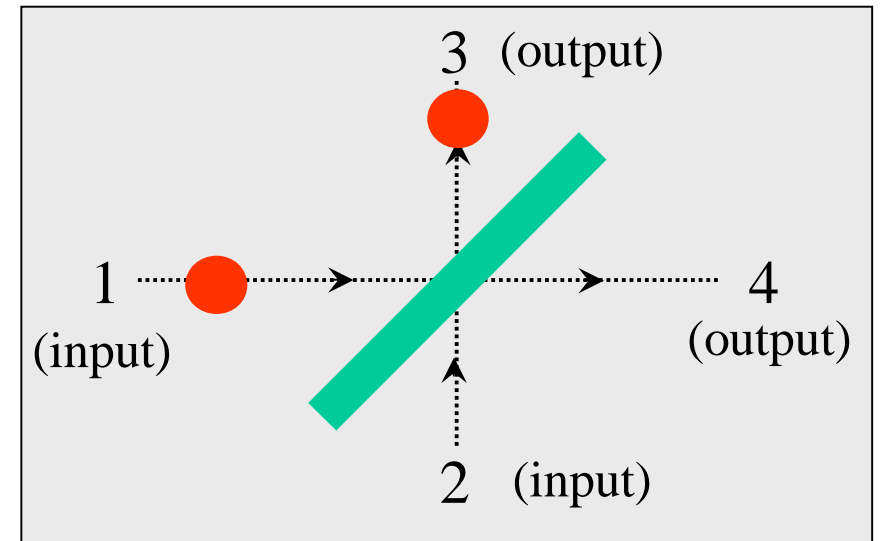


Photon coalescence

- One photon impinges on beam-splitter

$$|1_1\rangle / |0_2\rangle \longrightarrow r |1_3\rangle / |0_4\rangle + t |0_3\rangle / |1_4\rangle$$

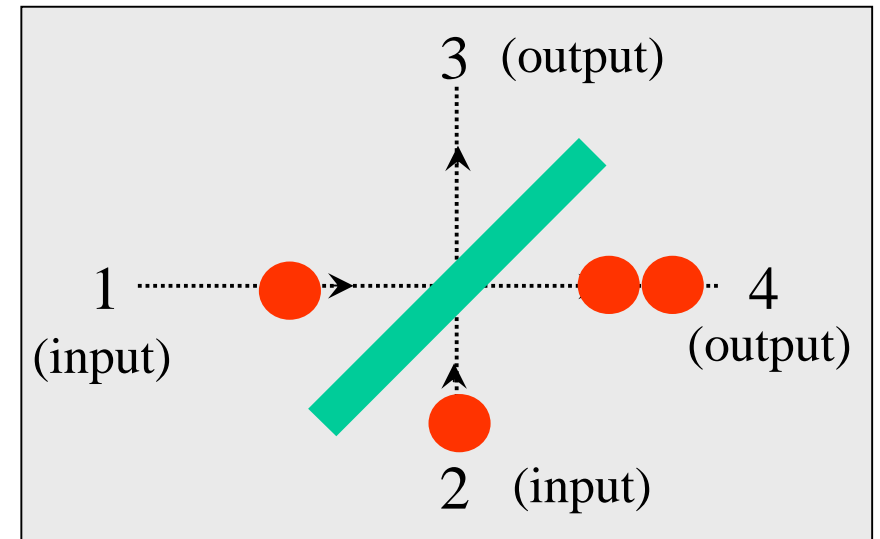
$$|0_1\rangle / |1_2\rangle \longrightarrow t |1_3\rangle / |0_4\rangle - r |0_3\rangle / |1_4\rangle$$



- Two photons impinge on beam-splitter

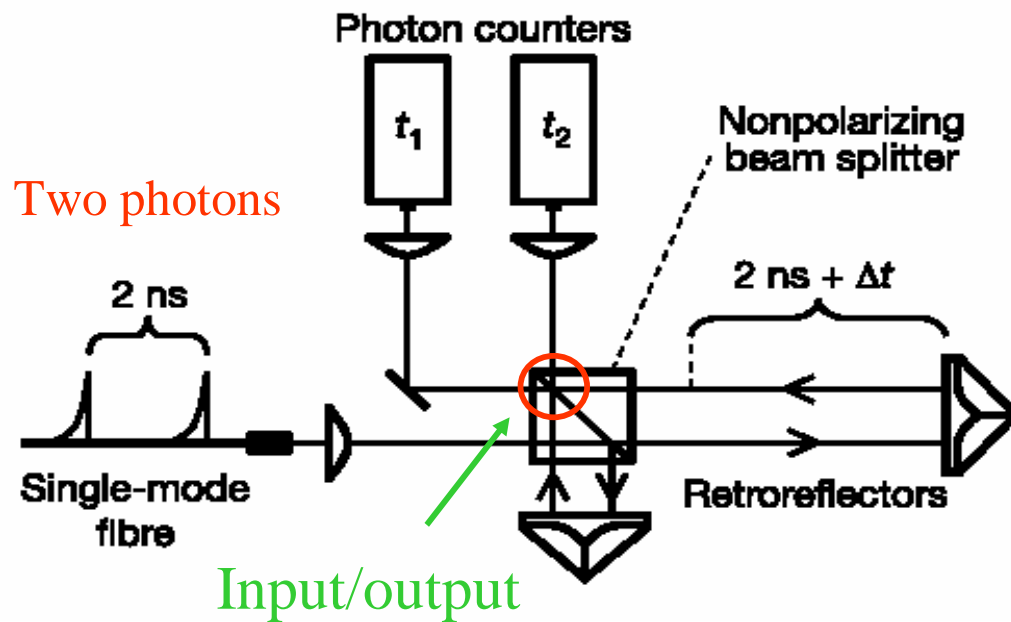
$$\begin{aligned} & |1_1\rangle / |1_2\rangle \\ & \downarrow \\ & t^2 |1_3\rangle / |1_4\rangle - r^2 |1_3\rangle / |1_4\rangle \\ & + rt |2_3\rangle / |0_4\rangle - rt |0_3\rangle / |2_4\rangle \end{aligned}$$

if $r = t$, only two-photon states



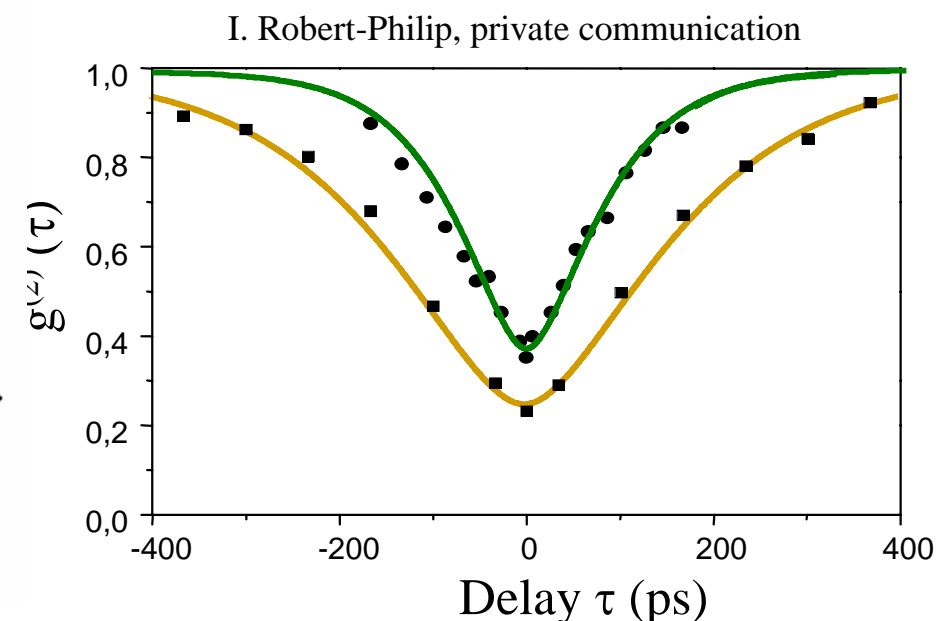
Indistinguishable photons

- Coalescence requires generation of **two indistinguishable photons**



Santori, Nature **419**, 594 (2002)

Sequential emission from the same QD



No coincidence :
coalescence of the two photons



Single-mode single-photon emission

AND ALSO

- Quantum teleportation Fattal, PRL **92**, 037904 (2004)
- Bell's inequality violation Fattal, PRL **92**, 037903 (2004)

Demonstration of single-mode single-photon emission
(polarization, space, spectrum) from a single QD

see also Moreau, APL **79**, 2865 (2001)

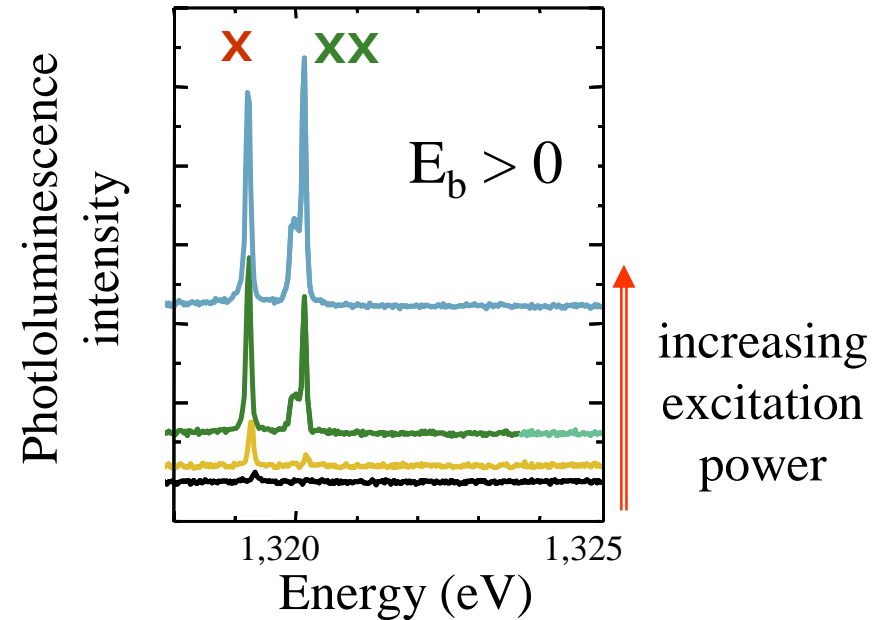
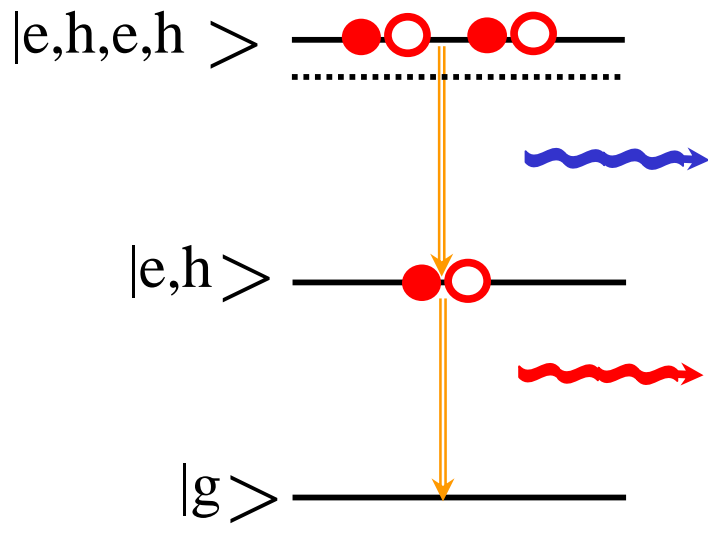


Single QD as two-photon source



Exciton and biexciton

- two (e,h) pairs are photogenerated in a single QD



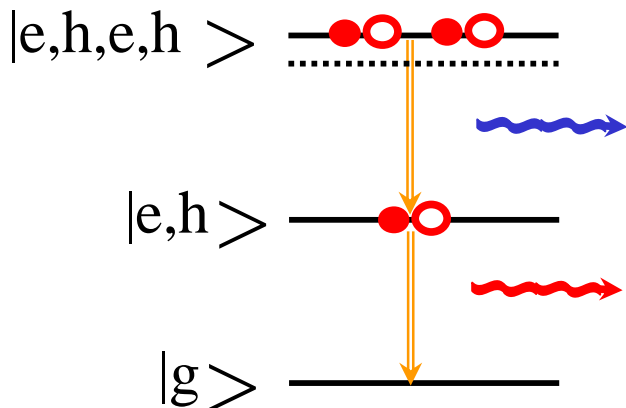
- Coulomb correlated state with 1 (e,h) pair = **exciton** (X)
- Coulomb correlated state with 2 (e,h) pairs = **biexciton** (XX)

$$E_{XX} = 2E_X + E_b$$

binding energy



Carrier quantum cascade

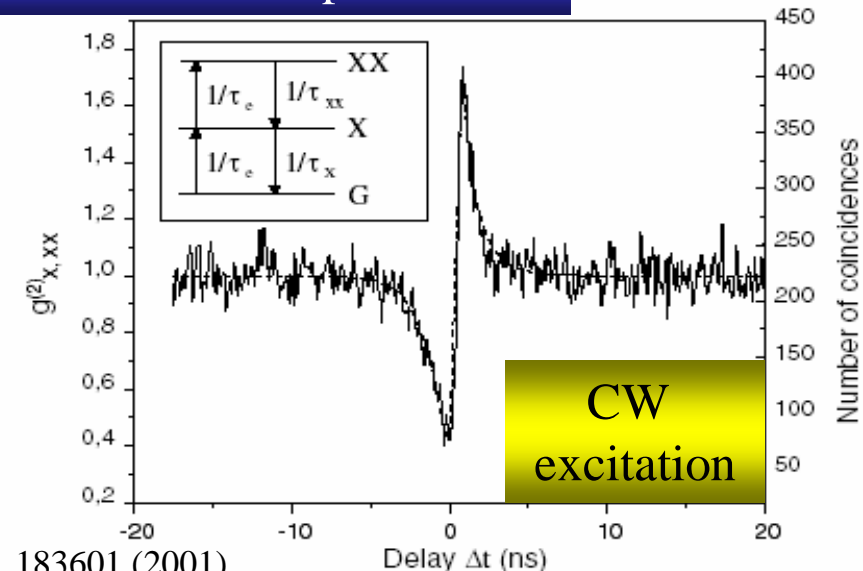
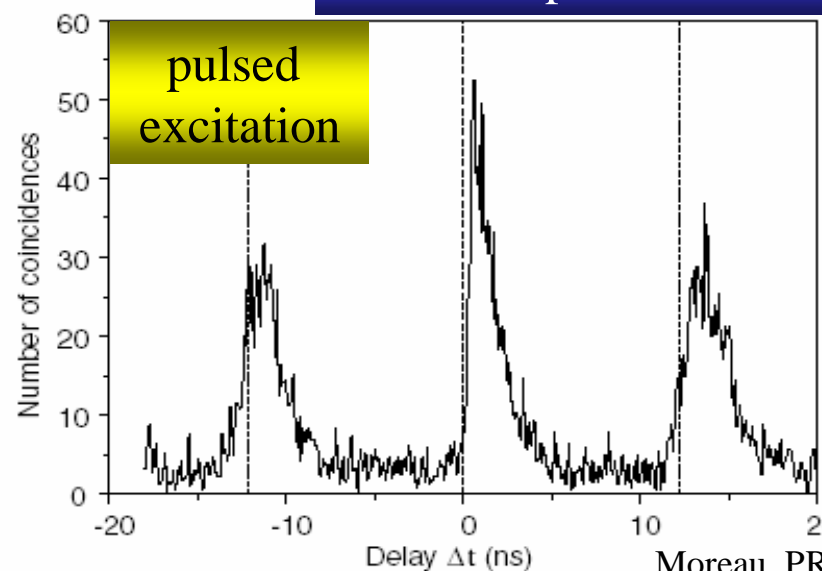


Two-color correlation experiments

XX photon on Start photodiode

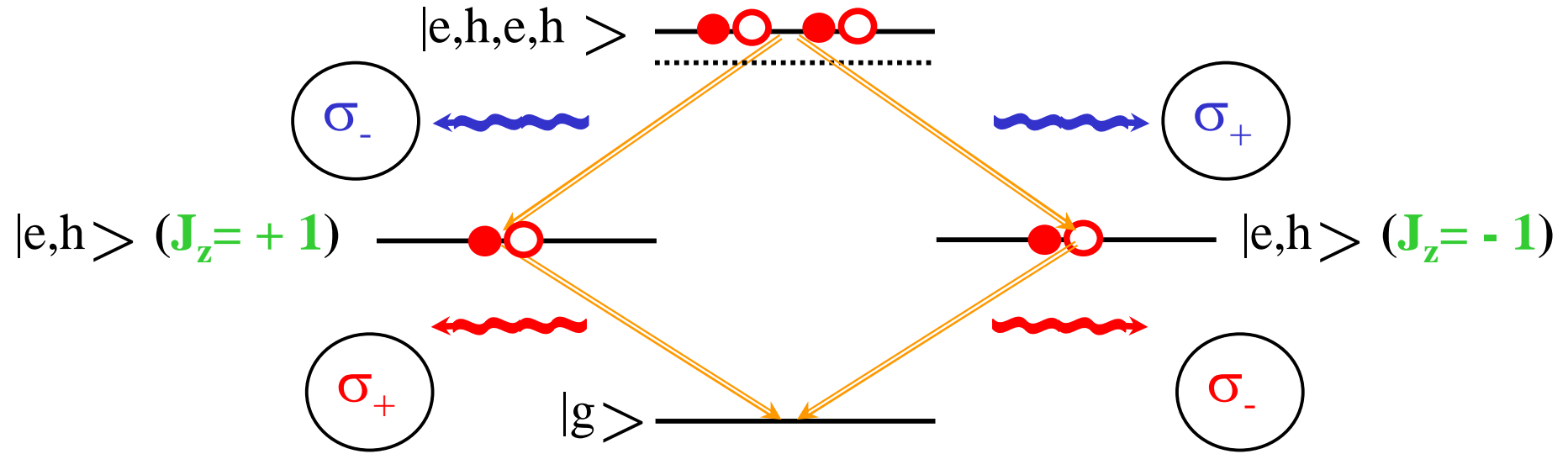
X photon on Stop photodiode

Biexciton photon is emitted before exciton photon



Bell states generation

- Fundamental transition **degeneracy**



- Two parallel paths possible generation of **entangled photon states**

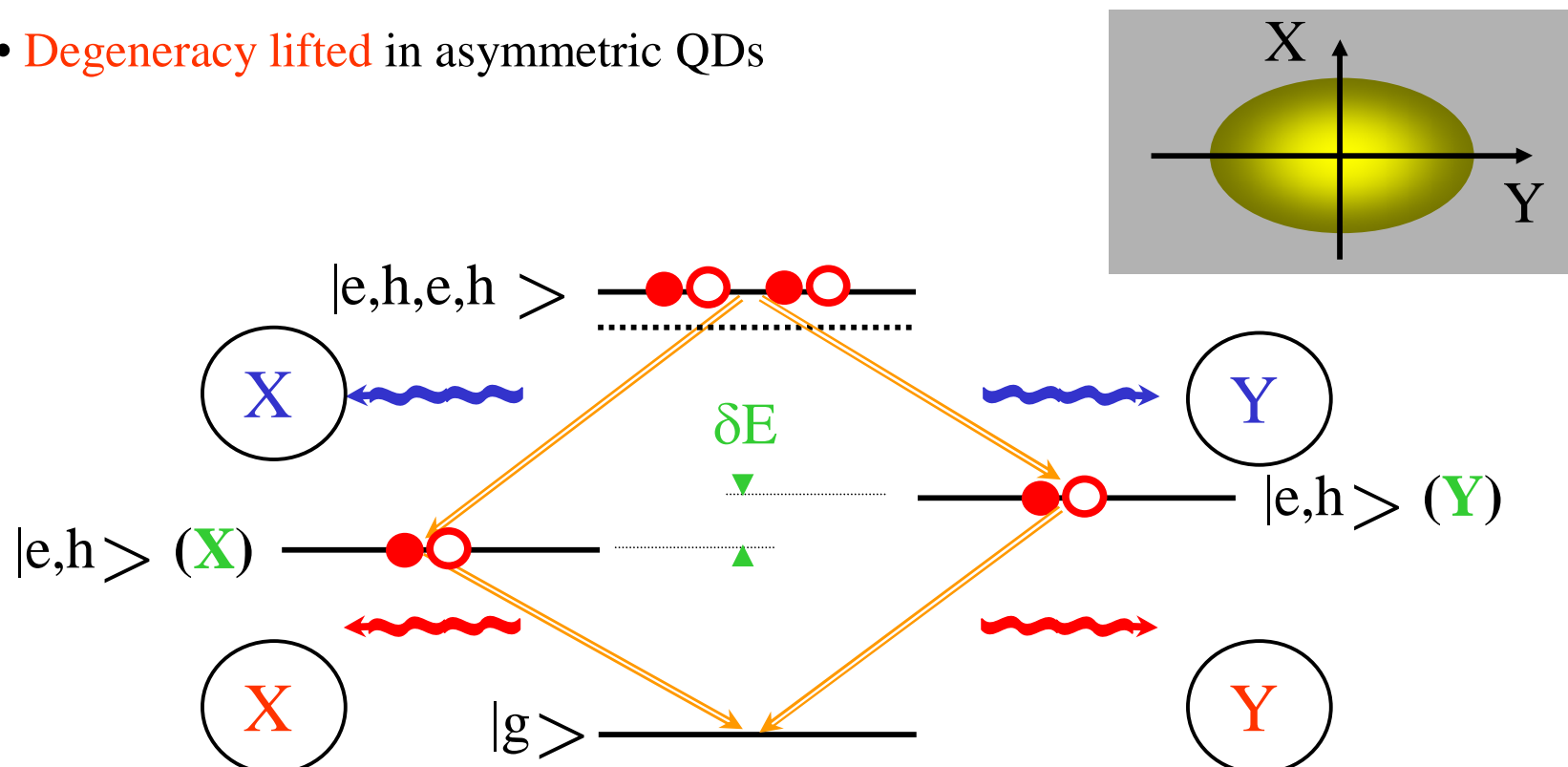
$$|\psi\rangle = \frac{|\sigma_-\rangle_{xx}|\sigma_+\rangle_x + |\sigma_+\rangle_{xx}|\sigma_-\rangle_x}{\sqrt{2}} \neq |\phi\rangle_{xx}|\phi\rangle_x$$

Benson, PRL **84**, 2513 (2000)



Rotational symmetry breaking

- Degeneracy lifted in asymmetric QDs



- Observation of polarization correlations but not entanglement

if $\delta E \gg \Gamma_X, \Gamma_Y$

Santori, PRB **66**, 045308 (2002)



Towards efficient single photon sources

All these experiments are performed at low temperature ($T \sim 5-10K$)
to avoid phonon-assisted dephasing processes

All these experiments use single QDs embedded in micropillar to
control spontaneous emission



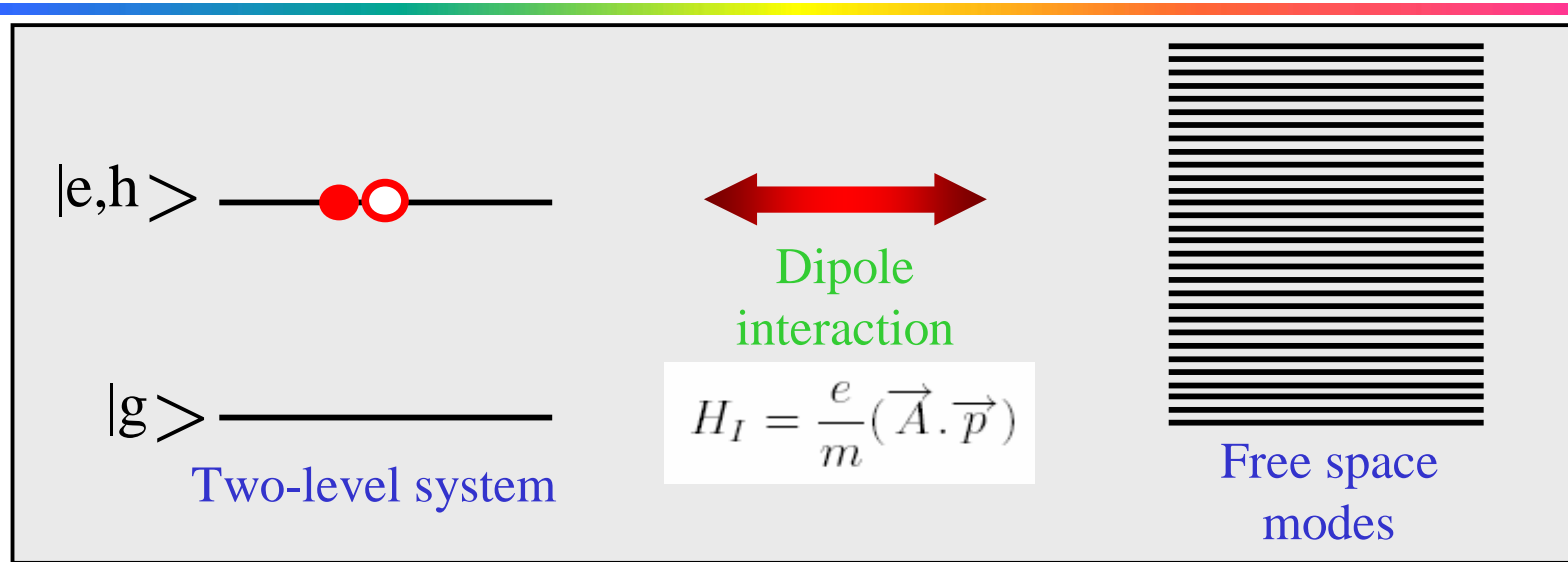
Spontaneous emission control

Outline

- Fermi's golden rule
- Purcell effect
- from weak to strong coupling



Fermi's golden rule



- Time domain analysis

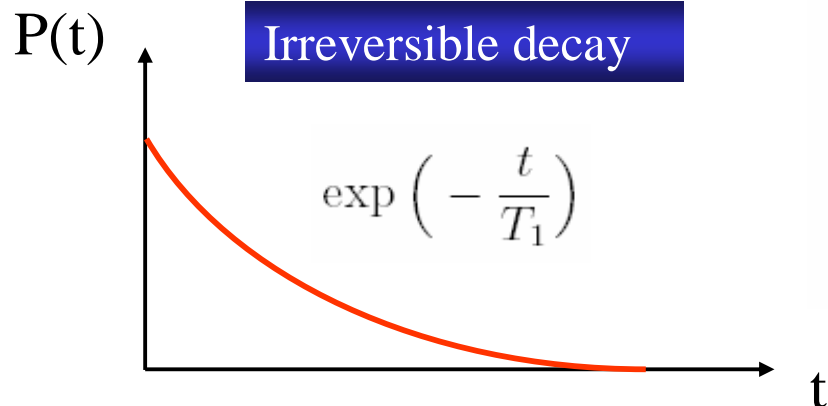
$$|i\rangle = |e, h\rangle |0_\omega\rangle \quad |f\rangle = |g\rangle |1_\omega\rangle$$

$$P_{|i\rangle}(t) = \exp\left(-\frac{t}{T_1}\right)$$

where $\frac{1}{T_1} = \frac{2\pi}{\hbar} \sum_{\{|1_\omega\rangle\}} |\langle f | \widetilde{H}_I | i \rangle|^2 \delta(E_{|e,h\rangle} - \hbar\omega)$



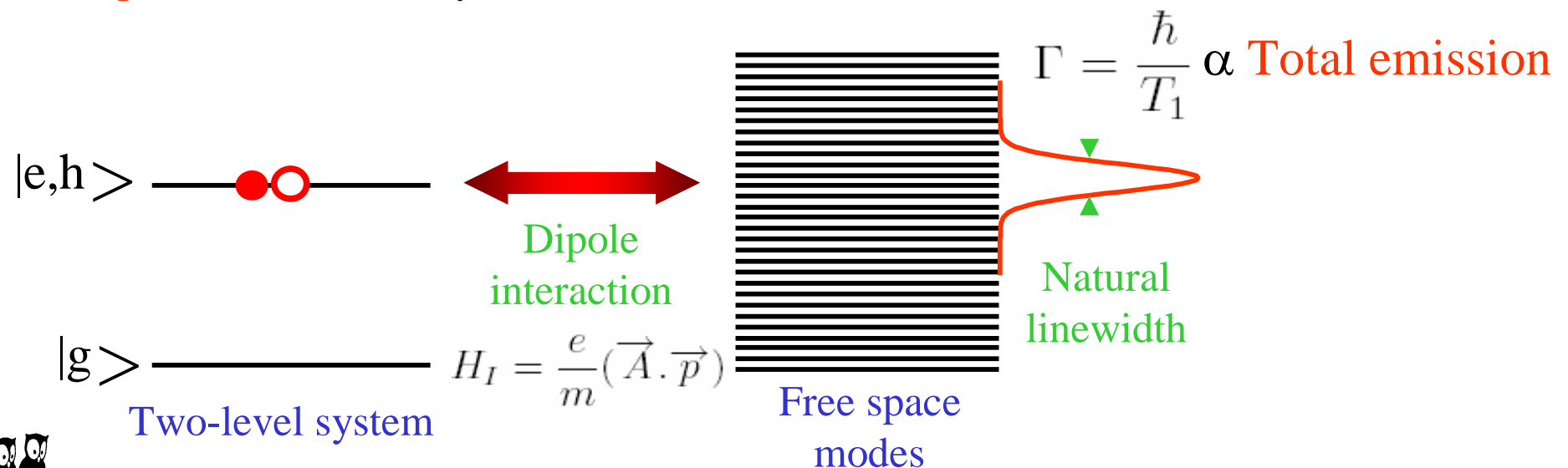
Natural linewidth



- Spectral domain analysis

$$\begin{aligned} \frac{1}{T_1} &\sim \frac{2\pi}{\hbar} |\langle f | \widetilde{H}_I | i \rangle|^2 \sum_{\{|1_\omega\rangle\}} \delta(E_{|e,h\rangle} - \hbar\omega) \\ &\sim \frac{2\pi}{\hbar} |\langle f | \widetilde{H}_I | i \rangle|^2 \underbrace{\rho_{e.m.}(E_{|e,h\rangle})}_{\text{free-space density of electromagnetic modes}} \end{aligned}$$

free-space density of
electromagnetic modes

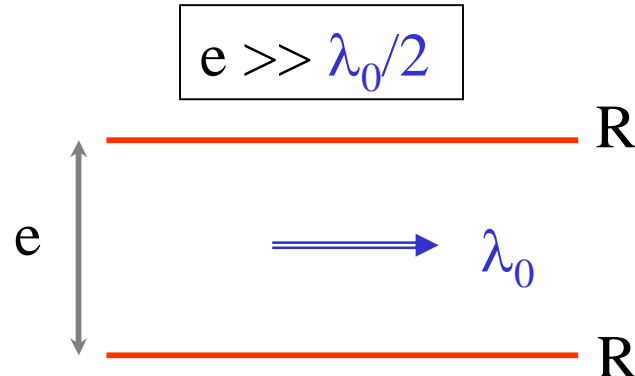


From free-space to cavities



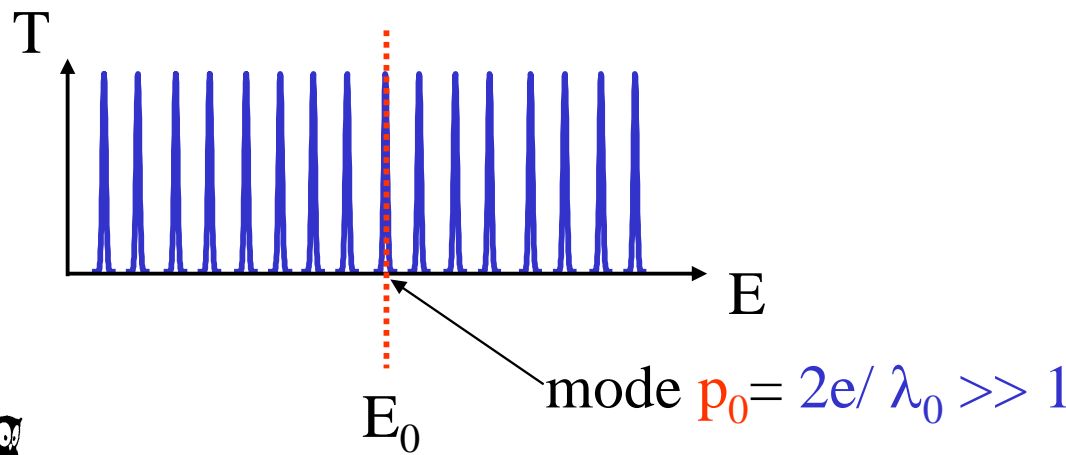
Fabry-Pérot cavity

- Fabry-Pérot cavity with **metallic mirrors**



$$\nu_p = p \frac{c}{2e} \frac{1}{\cos(\theta_p)}$$
$$E_p = E_0 \frac{\lambda_0/2}{e} \frac{p}{\cos(\theta_p)} \quad \text{with} \quad E_0 = \frac{hc}{\lambda_0}$$

- Fabry-Pérot transmission at **normal incidence**



- Free spectral range

$$\frac{E_0}{p_0}$$

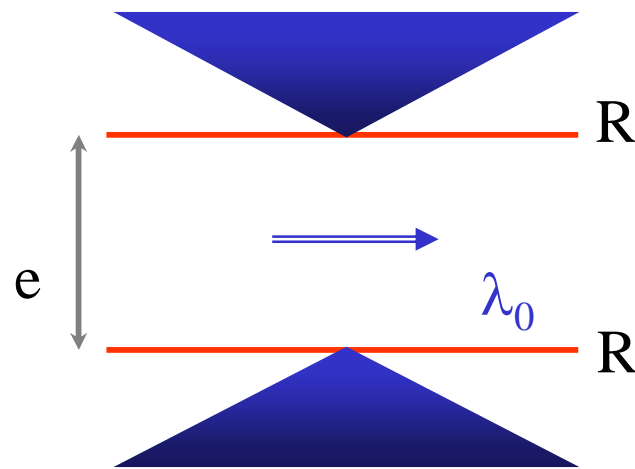
- for **large** cavities

$$\frac{E_0}{p_0} \ll E_0$$



Angular redistribution in planar cavities

$$e \gg \lambda_0/2, p_0 \gg 1$$



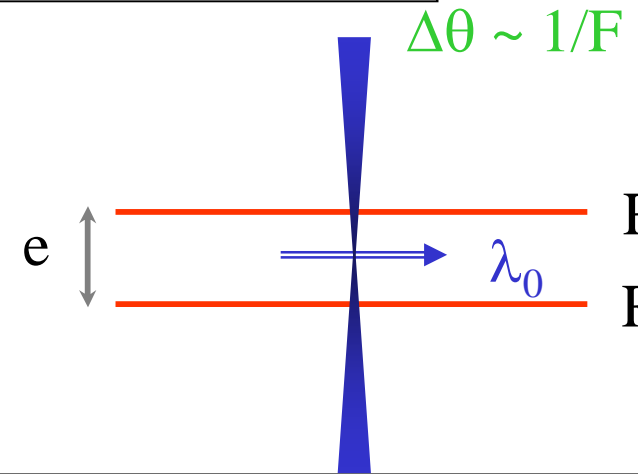
$$E_p = E_0 \frac{p/p_0}{\cos(\theta_p)}$$

resonant interaction of emitter with a large number of modes at different emission angles



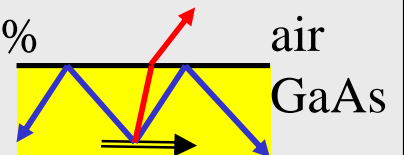
A. Kastler, Appl. Optics 1,17 (1962)

$$e = \lambda_0/2, p_0 = 1$$



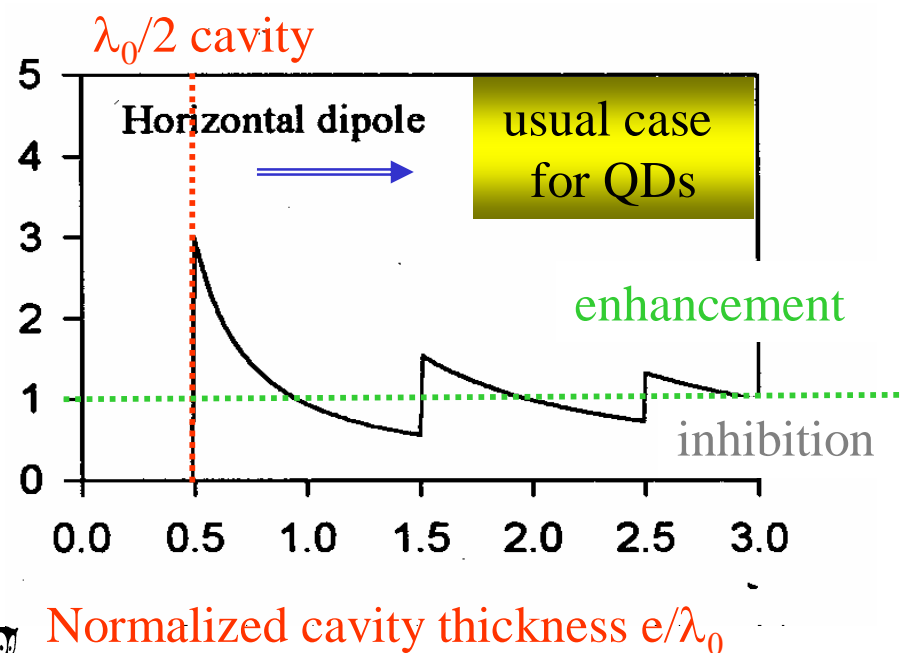
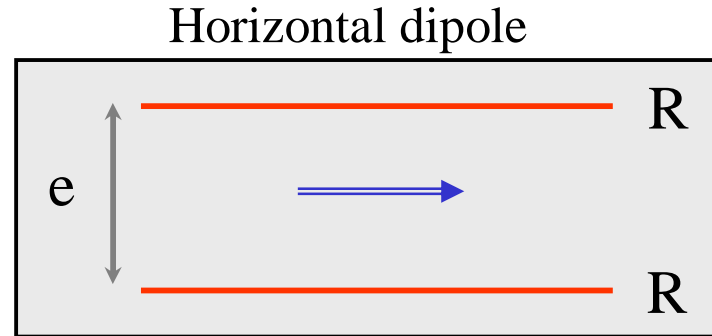
- resonant interaction of emitter with a single mode
- angular redistribution of the dipole emission
- enhanced extraction efficiency $\eta \sim 25\%$

Total internal reflection $\eta \sim 2\%$
for $i > 13^\circ$



Enhancement and inhibition

Brorson, IEEE JQE **26**, 1492 (1990)



$$\frac{1}{T_1} \sim \frac{2\pi}{\hbar} |\langle f | \widetilde{H}_I | i \rangle|^2 \rho_{e.m.}(E_{|e,h\rangle})$$

- free space $E = \hbar c k$

$$\rho_{3D}(E) = \frac{\Omega}{\pi^2} \frac{E^2}{(\hbar c)^3}$$

- $\lambda_0/2$ cavity

$$E = \hbar c \sqrt{\left(\frac{\pi}{e}\right)^2 + k_{\parallel}^2} \quad [E_0, 2E_0]$$

$$\rho_{2D}(E) = \frac{2\Sigma}{\pi} \frac{E}{(\hbar c)^2}$$

for $\lambda_0/2$ cavity

$$\frac{\rho_{2D}(E_0)/(e\Sigma)}{\rho_{3D}(E_0)/\Omega} = 2$$

??



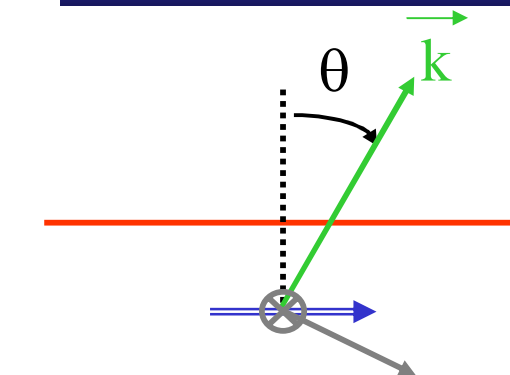
Dipole-field orientation

$$\frac{1}{T_1} = \frac{2\pi}{\hbar} \sum_{\{|1_\omega\rangle\}} |\langle f | \widetilde{H}_I | i \rangle|^2 \delta(E_{|e,h\rangle} - \hbar\omega)$$

mode-dependent term in matrix element

$$\vec{A} \cdot \langle u_c | \vec{p} | u_v \rangle = \vec{A} \cdot \vec{P}_{cv} = AP_{cv} \cos \alpha$$

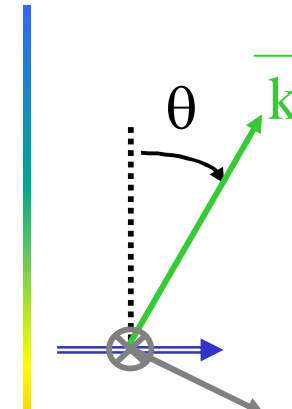
Fabry-Pérot cavity



given E \rightarrow single angle θ

two modes $\begin{cases} \alpha = \pi/2 \\ \alpha = \theta \end{cases}$

1/2



Free space

given E \rightarrow $\theta : [0, \pi]$

two modes $\begin{cases} \alpha = \pi/2 \\ \alpha = \theta \end{cases}$

1/2

$$\int_0^\pi \cos^2 \theta \sin \theta d\theta d\varphi = \frac{2}{3} d\varphi$$

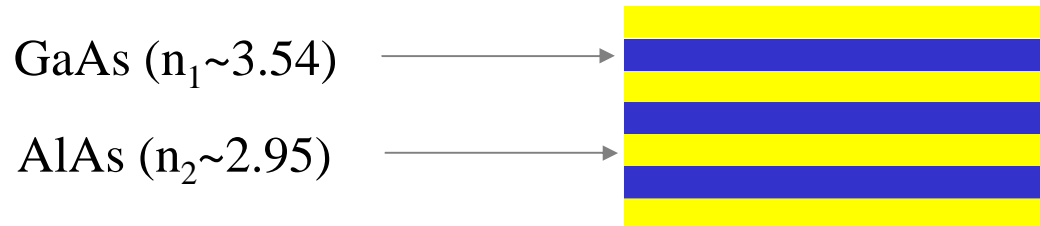
for $\lambda_0/2$ cavity

$$\frac{\rho_{2D}(E_0)/(e\Sigma) * 1/2}{\rho_{3D}(E_0)/\Omega * 1/3} = 3$$



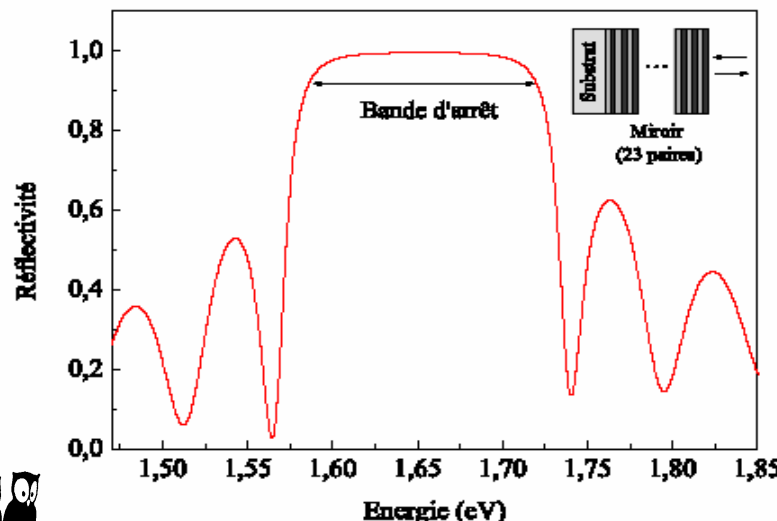
Semiconductor microcavities

- metallic mirrors = **lossy** at optical frequencies
- epitaxially grown **Distributed Bragg Reflectors**

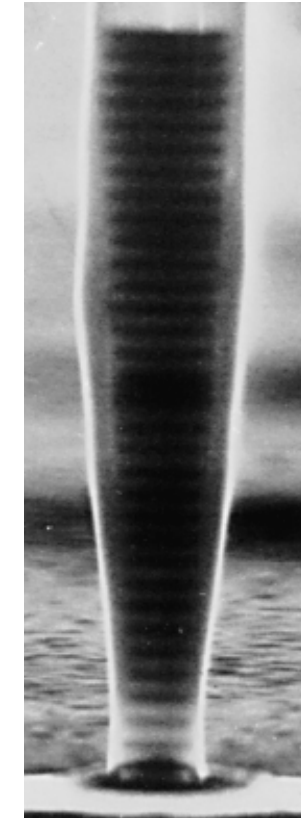


stacked pairs of GaAs/AlAs with $n_1 e_1 = n_2 e_2 = \lambda_0 / 4$

- **reflectivity spectrum**



- **High** reflectivity
 $R_{\max} \sim 99.5\%$
with 23 pairs
- **Stop-band** width ΔE
 $\Delta E/E_0 \sim (n_1 - n_2)/\langle n \rangle$

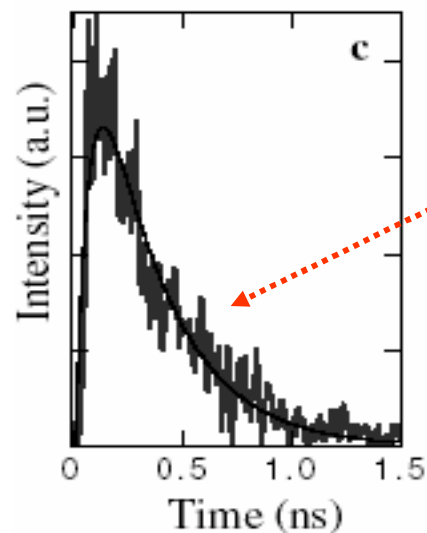


Gérard, PRL 81, 1110 (1998)



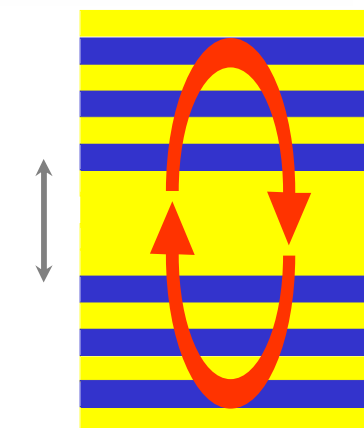
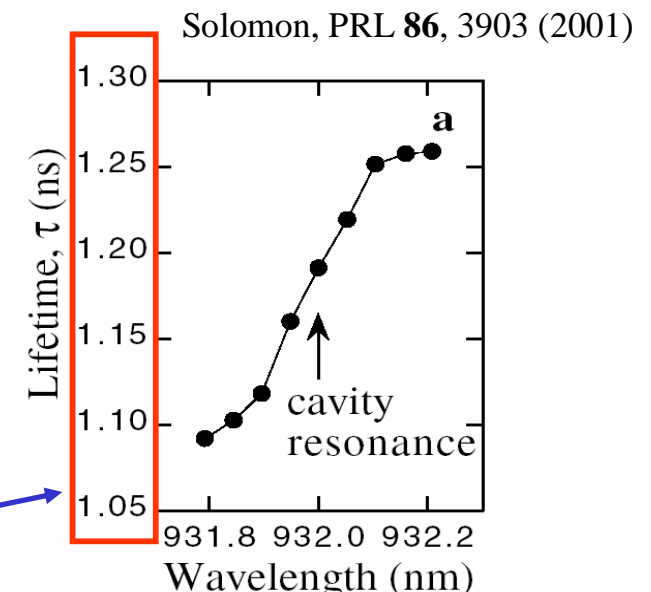
QDs in planar semiconductor microcavities

- time-resolved photoluminescence experiments



+/- 10%

- very weak effect on QD spontaneous emission dynamics !
- in DBR based-cavity, the effective cavity length ne is around $4\lambda_0$

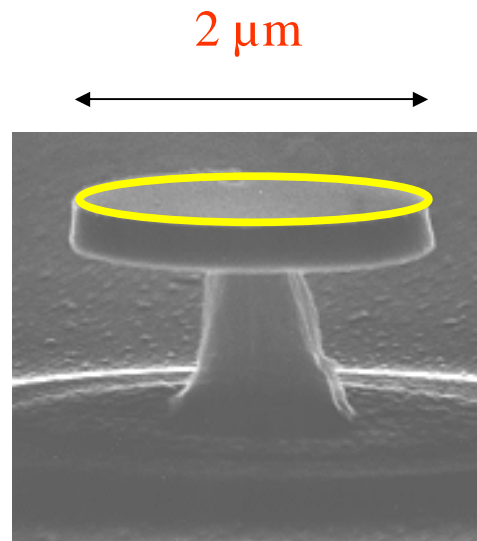


Some solid-state 0D microcavities



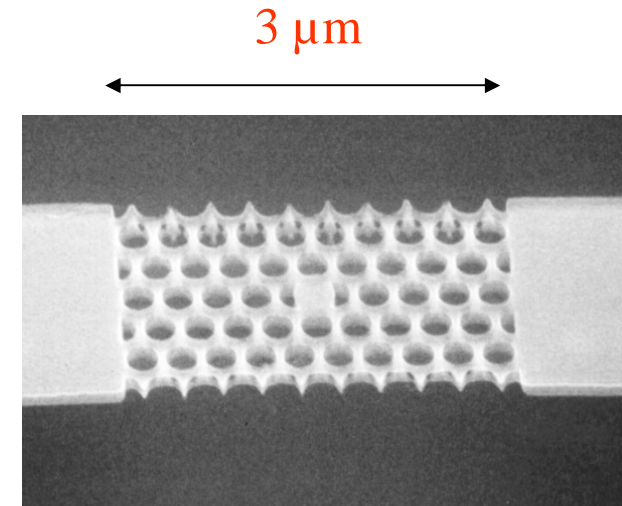
Micropillars

lateral etching
of planar
semiconductor
DBRs

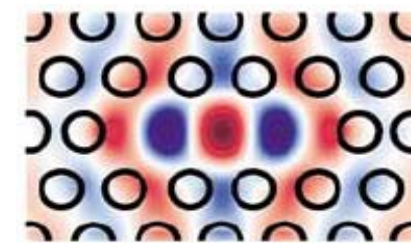


Microdisks

whispering
gallery modes



Photonic crystals defects



Akahane, Nature 425, 944 (2003)

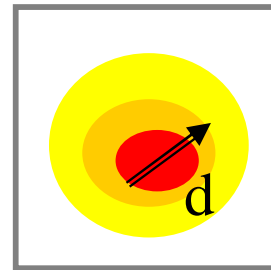


Two important figures of merit

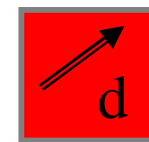
- spatial confinement of electromagnetic field

V_{eff} :
effective
mode volume

$$\varepsilon_{max} = \sqrt{\frac{\hbar\omega}{2\varepsilon_0 n^2 V_{eff}}}$$



Actual cavity



Equivalent cavity
volume V_{eff}

- temporal confinement of electromagnetic field

Q :
mode
quality factor

$$Q = \frac{E_0}{\Gamma_{cav}} \longrightarrow \tau_{photon} = \frac{\hbar}{\Gamma_{cav}}$$

around 1 eV, $Q = 1000$ photon = 0.6 ps



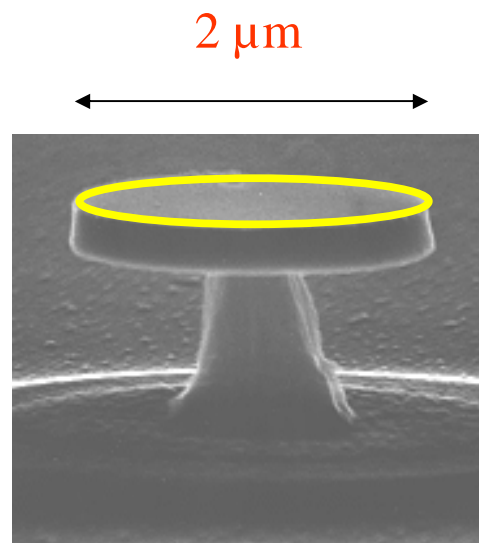
High-Q small-mode volume 0D cavities



Micropillars

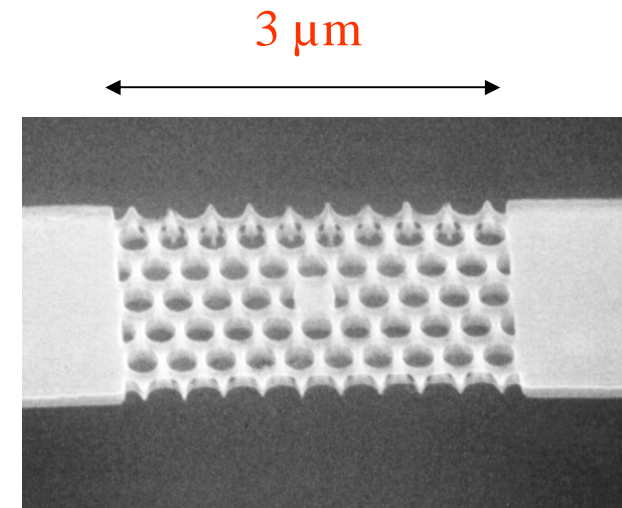
$$V=5 (\lambda/n)^3$$
$$Q \sim 7000$$

Reithmaier, Nature **432**, 197 (2004)



Microdisks

$$V=6 (\lambda/n)^3$$
$$Q \sim 12000$$



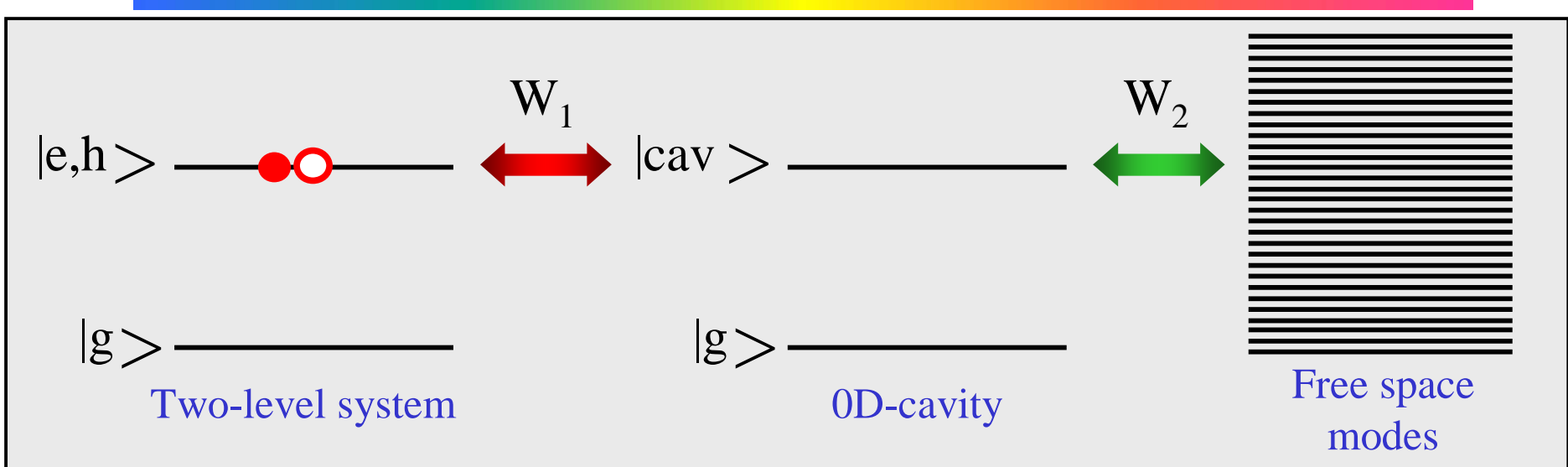
Photonic crystals defects

$$V=1.2(\lambda/n)^3$$
$$Q \sim 20000$$

Yoshie, Nature **432**, 200 (2004)



Quasi-mode approximation



- two cases : $W_1 > W_2$ strong coupling regime
 $W_1 < W_2$ weak coupling regime
- in the weak coupling regime, QD is coupled to the electromagnetic field which mode density is given by :

$$\rho(E) = \frac{2Q}{\pi E_{cav}} \frac{E_{cav}^2}{4Q^2(E - E_{cav})^2 + E_{cav}^2}$$

damped 0D-cavity mode
= quasi-mode

Fano, Phys. Rev. **124**, 1866 (1961)



Purcell factor

$$\frac{1}{T_1} = \frac{2\pi}{\hbar} \sum_{\{|1_\omega\rangle\}} |\langle f | \widetilde{H}_I | i \rangle|^2 \delta(E_{|e,h\rangle} - \hbar\omega)$$

with $\vec{A}(\vec{r}) = i\sqrt{\frac{\hbar}{2\varepsilon_0\omega V_{eff}}} (a\vec{f}^*(\vec{r}) + a^+\vec{f}(\vec{r}))$ where $\begin{cases} \left|\vec{f}(\vec{r})\right|_{max} = 1 \\ \int d^3\vec{r} \left|\vec{f}(\vec{r})\right|^2 = V_{eff} \end{cases}$

free space

$$\left(\frac{1}{T_1}\right)_{free\ space} = \frac{\Gamma}{\hbar} = \frac{1}{3} \frac{P_{cv}^2}{\varepsilon_0} \frac{E_0}{\pi\hbar^2c^3}$$

0D cavity

- dipole at the field maximum
- dipole parallel to field
- $E_0 = E_{cav}$

$$\left(\frac{1}{T_1}\right)_{cav} = \frac{\Gamma_p}{\hbar} = 2 \frac{P_{cv}^2}{\varepsilon_0} \frac{\hbar Q}{E_0^2 V_{eff}}$$

Purcell factor

Purcell, Phys. Rev. **69**, 681 (1946)

$$F_p = \frac{\Gamma_p}{\Gamma}$$

and we find

$$F_p = \frac{3}{4\pi^2} \frac{\lambda_0^3 Q}{V_{eff}}$$



Purcell effect in 0D-cavity

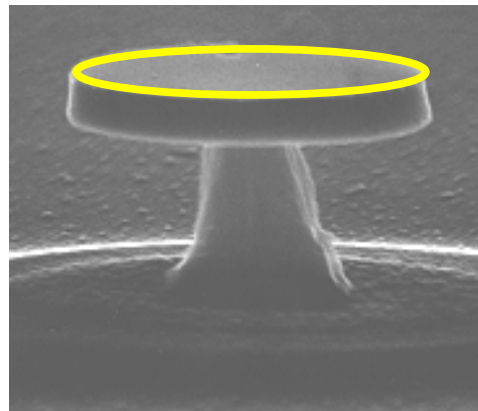
- QD = dipole in a dielectric 0D-cavity

$$F_p = \frac{3}{4\pi^2} \frac{(\lambda_0/n)^3 Q}{V_{eff}}$$

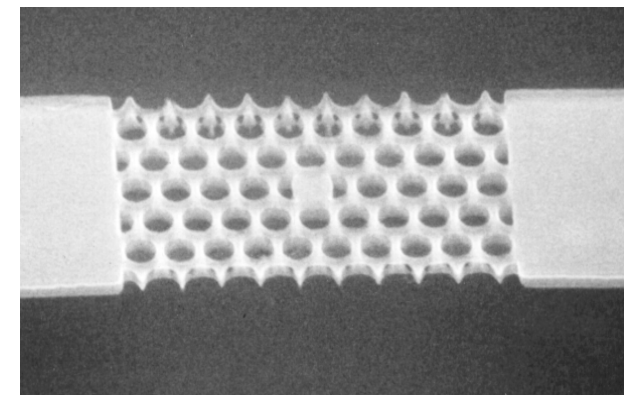
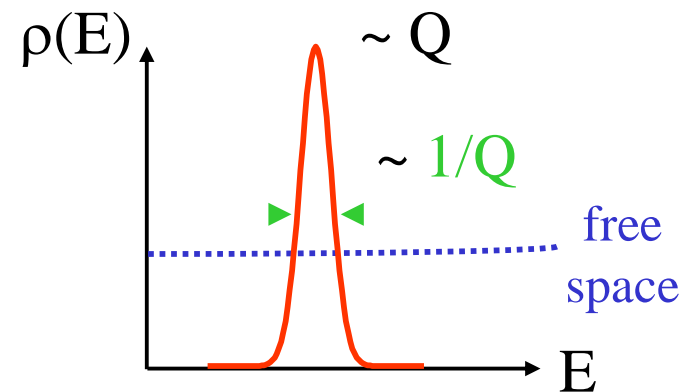
- Calculated Purcell factors



$V=5 (\lambda_0/n)^3$
 $Q \sim 7000$
 $F_p \sim 100$



$V=6 (\lambda_0/n)^3$
 $Q \sim 12000$
 $F_p \sim 150$



$V=1.2(\lambda_0/n)^3$
 $Q \sim 20000$
 $F_p \sim 800$

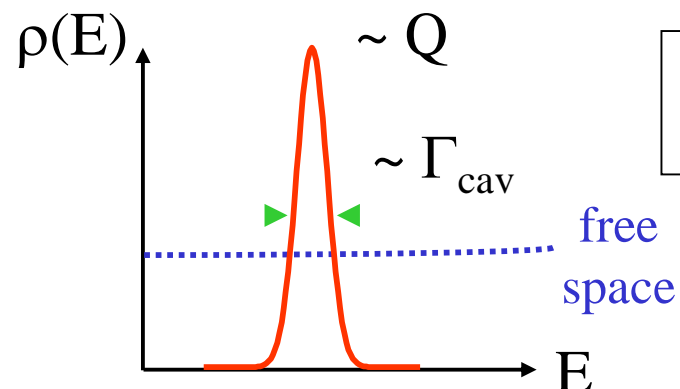


Purcell effect in a non-ideal case

$$F_p = F_p^0 \frac{E_{cav}^2}{4Q^2(E_0 - E_{cav})^2 + E_{cav}^2} \left| \vec{f}(\vec{r}_0) \right| \cos^2 \alpha$$

↑ ↑ ↑
 Spectral detuning Spatial detuning Dipole misorientation

- broadening of the QD emission line



no phonon-assisted dephasing

efficient
dephasing



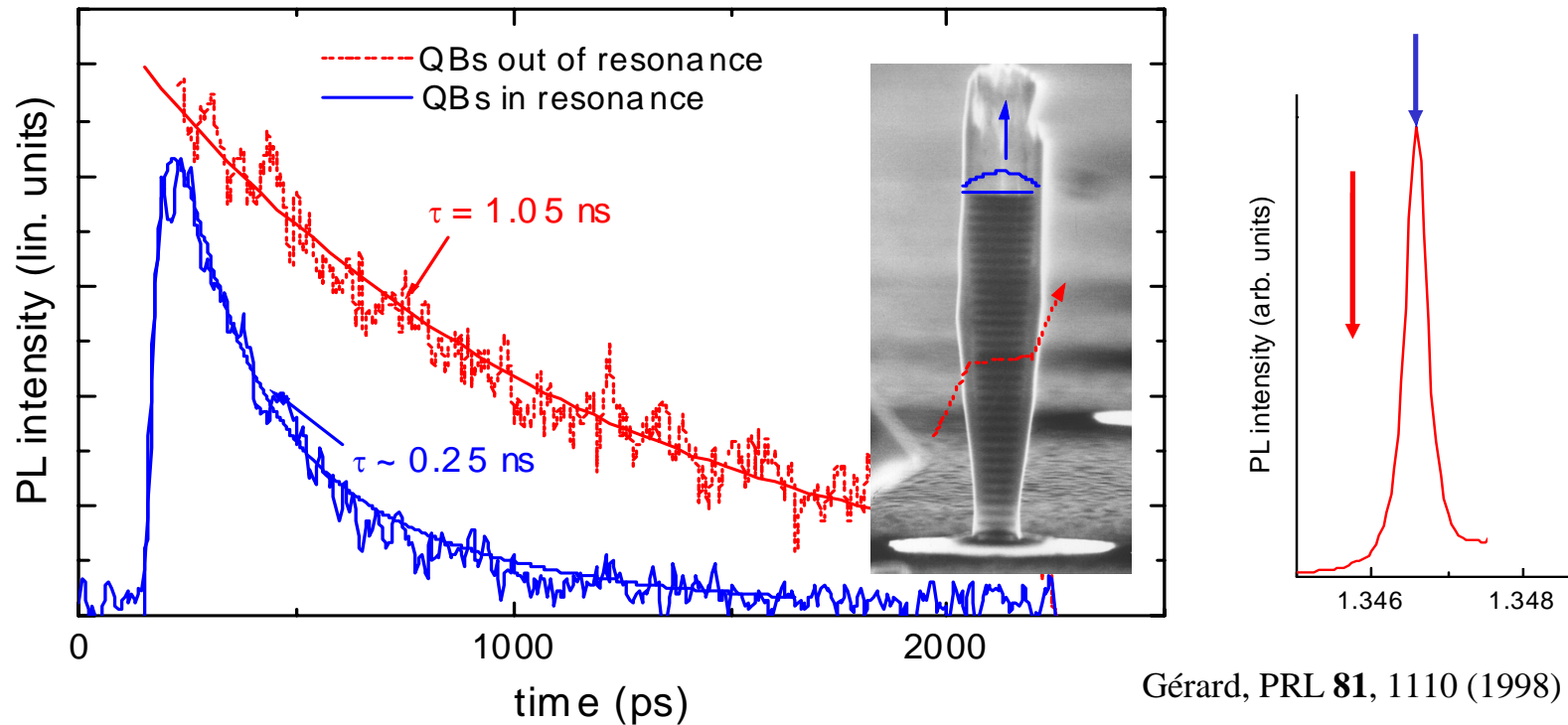
$$\rho(E) \longrightarrow \int du \rho(E-u) L_{\Gamma_{QD}}(u)$$

if $\Gamma_{QD} \gg \Gamma_{cav}$,
the Purcell effect is washed out



Purcell effect in InAs QDs

- time-resolved experiments in QD arrays : spatial + spectral averaging

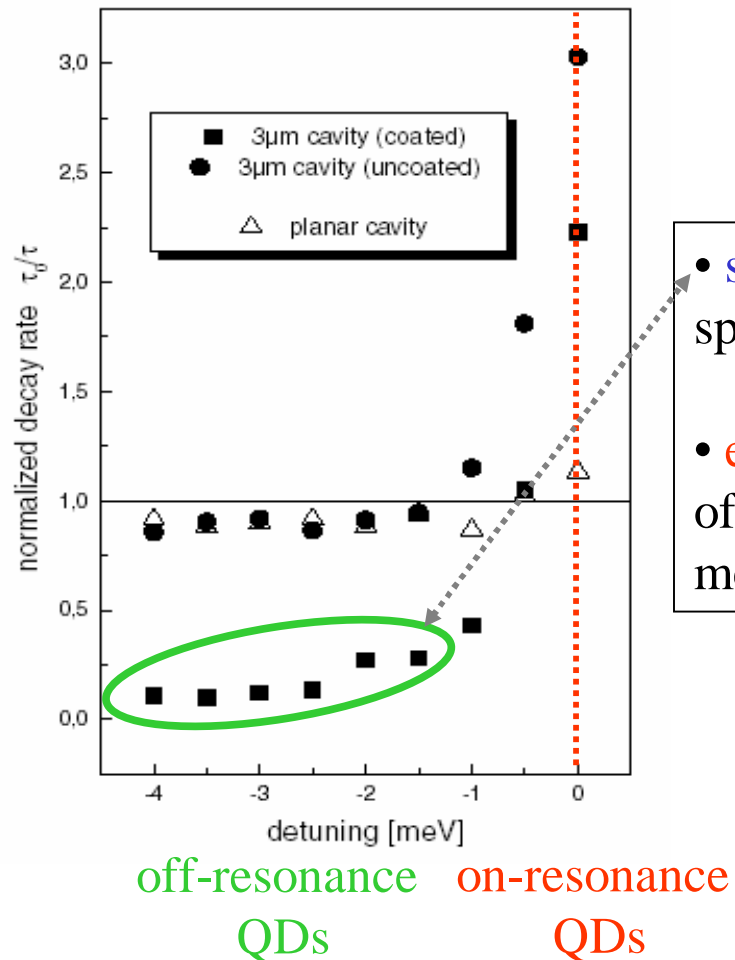


- PL decay **faster** only for **on-resonance** QDs : (x5) enhancement of spontaneous emission rate (much smaller than F_p)
- for **off-resonance** QDs, **free-space** like recombination dynamics : **leaky modes**



Spontaneous emission inhibition

- suppression of leaky modes in **gold-coated** micropillars



- strong inhibition (/10) of spontaneous emission rate
- efficient reduction of the density of non-resonant modes by the metallic coating

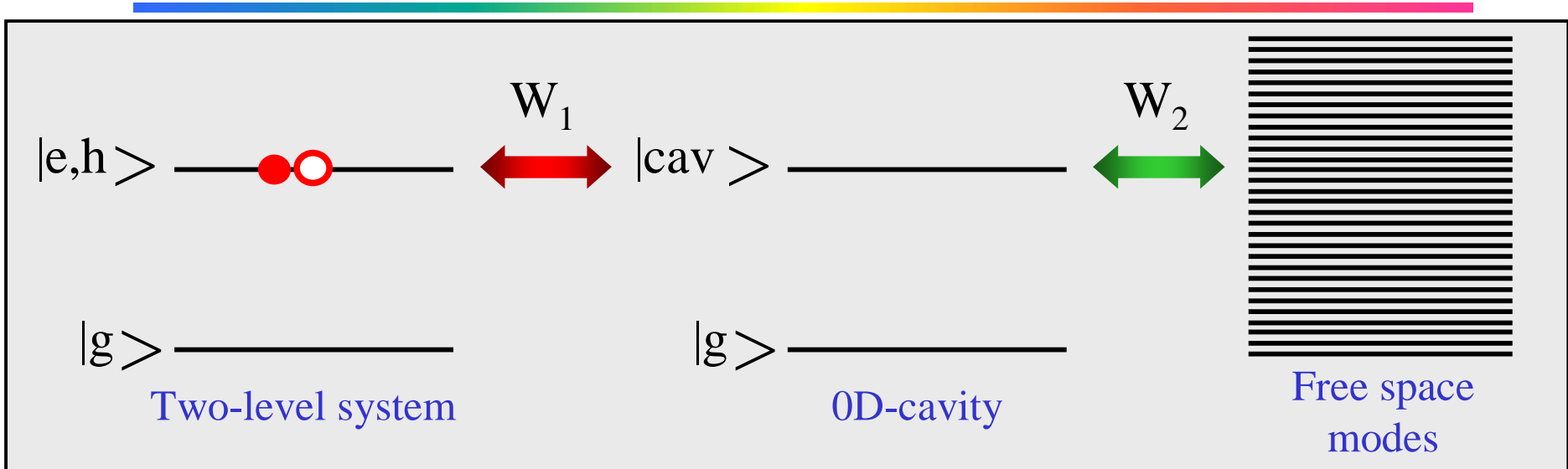
Bayer, PRL **86**, 3168 (2001)



Strong coupling regime



From weak to strong coupling



- two cases : $W_1 > W_2$ strong coupling regime
 $W_1 < W_2$ weak coupling regime
- in the strong coupling regime, the coupling to free space modes is a perturbation to (QD-cavity) sub-system

existence of mixed electron-photon states = microcavity polaritons



Microcavity polaritons

- two states of microcavity polariton

$$|-\rangle = \alpha |e, h\rangle + \beta |cav\rangle$$

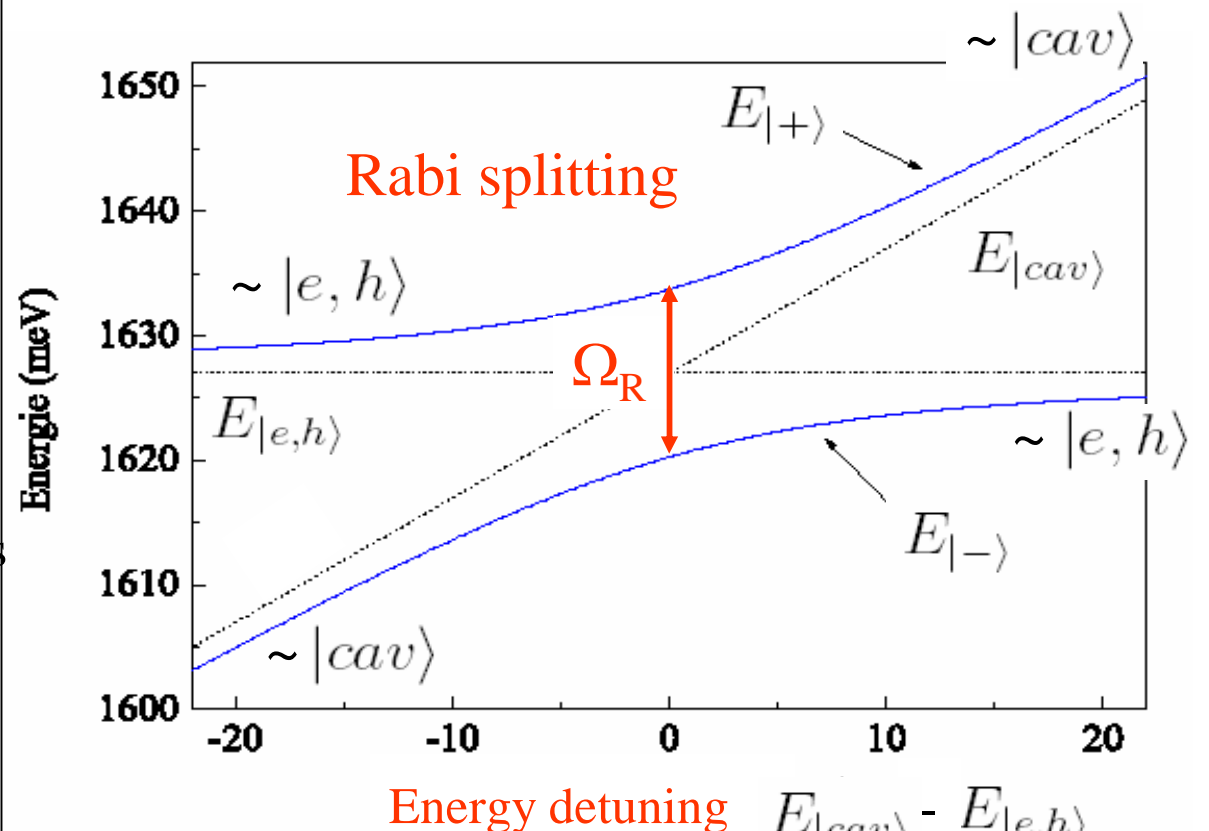
$$|+\rangle = \beta |e, h\rangle - \alpha |cav\rangle$$

- anti-crossing at zero detuning

$$E_{|+\rangle} - E_{|-\rangle} = \Omega_R$$

- at zero-detuning, the polaritons are half electron
half photon

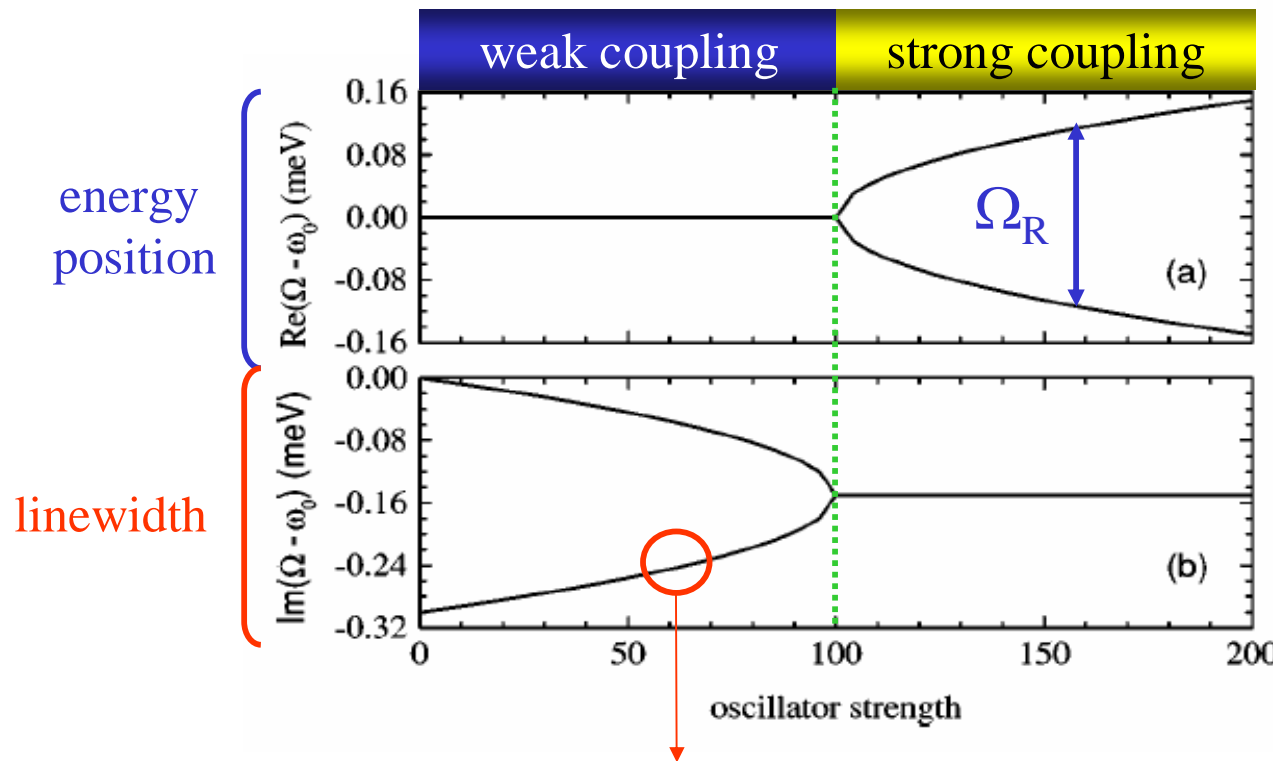
$$|\alpha|^2 = |\beta|^2 = \frac{1}{2}$$



Weak to strong coupling crossover

Andreani, PRB **60**, 13276 (1999)

$$\Omega_{\pm} = \omega_0 - \frac{i}{4}(\gamma_a + \gamma_{c,\mu}) \pm \sqrt{g^2 - \left(\frac{\gamma_a - \gamma_{c,\mu}}{4}\right)^2}$$



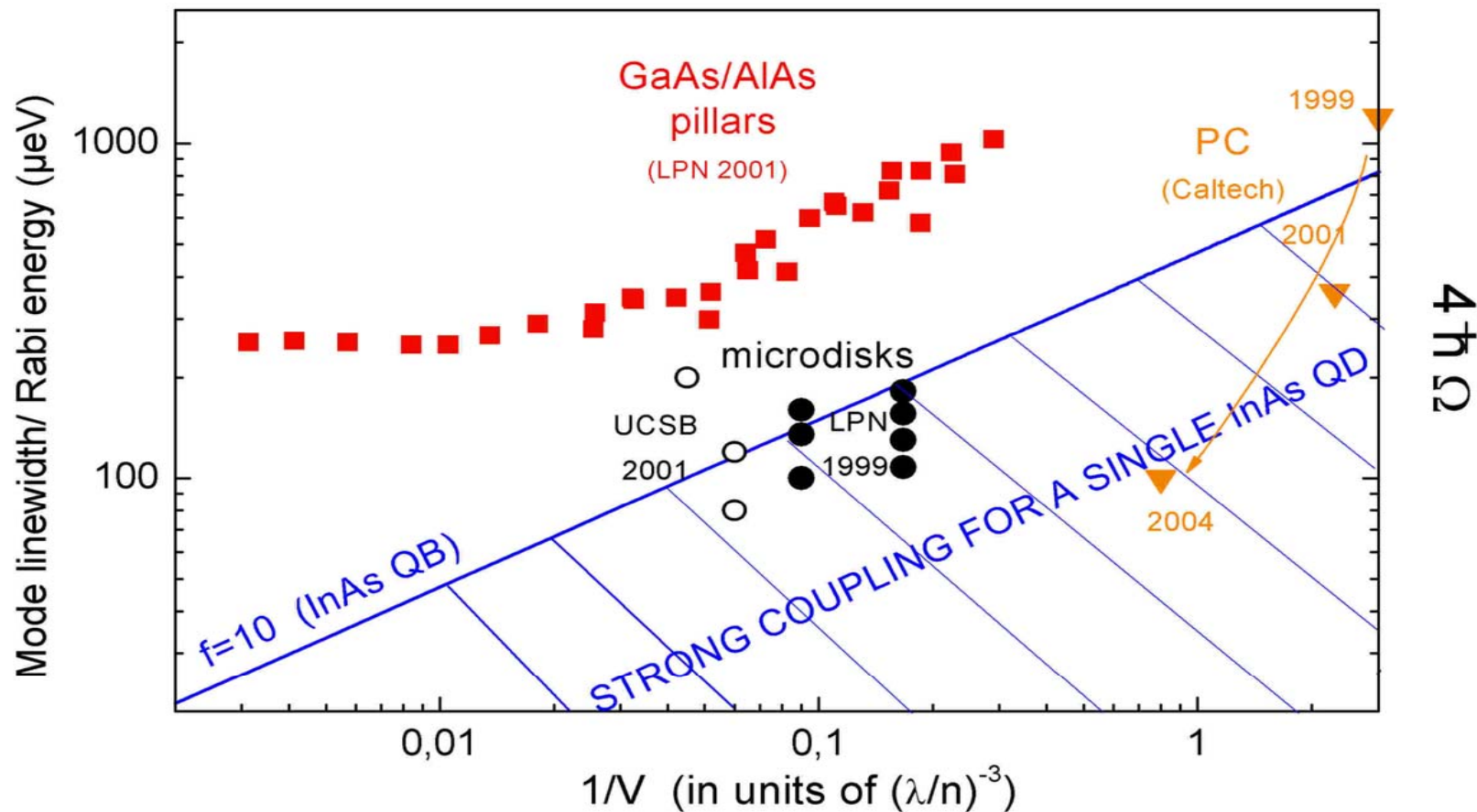
$\Gamma_p = F_p \Gamma$, modified spontaneous emission rate (Purcell effect)



$$\begin{aligned}\hbar g &\propto |\langle \vec{p}, \vec{A} \rangle| \propto \frac{1}{\sqrt{V_{\text{eff}}}} \\ \hbar \gamma_a &= \Gamma_{QD} \\ \hbar \gamma_{c,\mu} &= \Gamma_{cav} \propto \frac{1}{Q}\end{aligned}$$

weak coupling	$g \ll \gamma_a - \gamma_{c,\mu} $
high V_{eff}	small Q
strong coupling	$g \gg \gamma_a - \gamma_{c,\mu} $
small V_{eff}	high Q

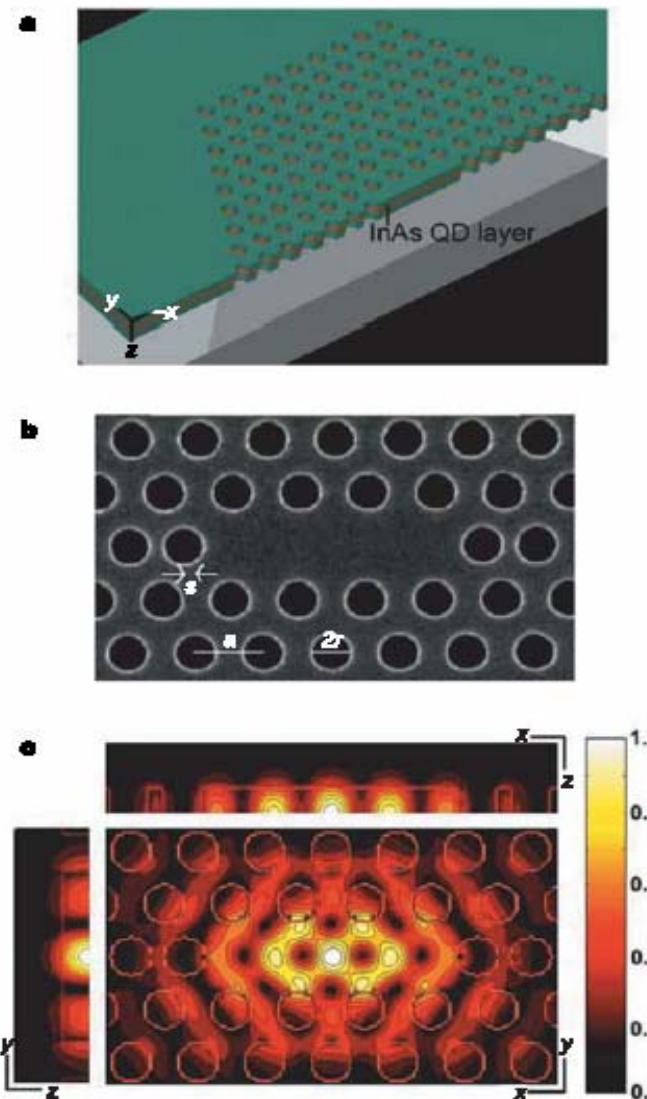
Towards strong coupling for a single QD



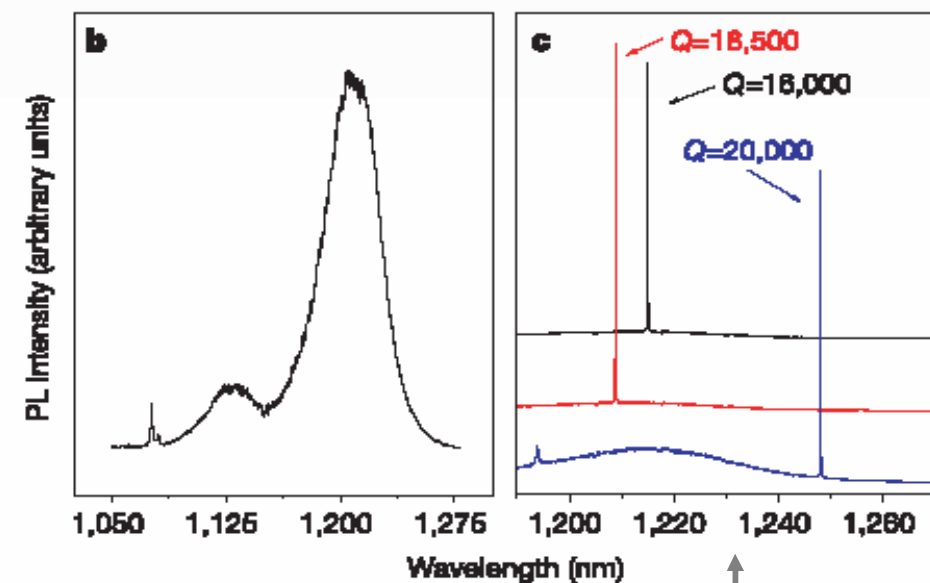
For a single InAs QD, strong coupling already observable with microdisks and PC cavities



Photonic crystals high-Q microcavities



Yoshie, Nature 432, 200 (2004)

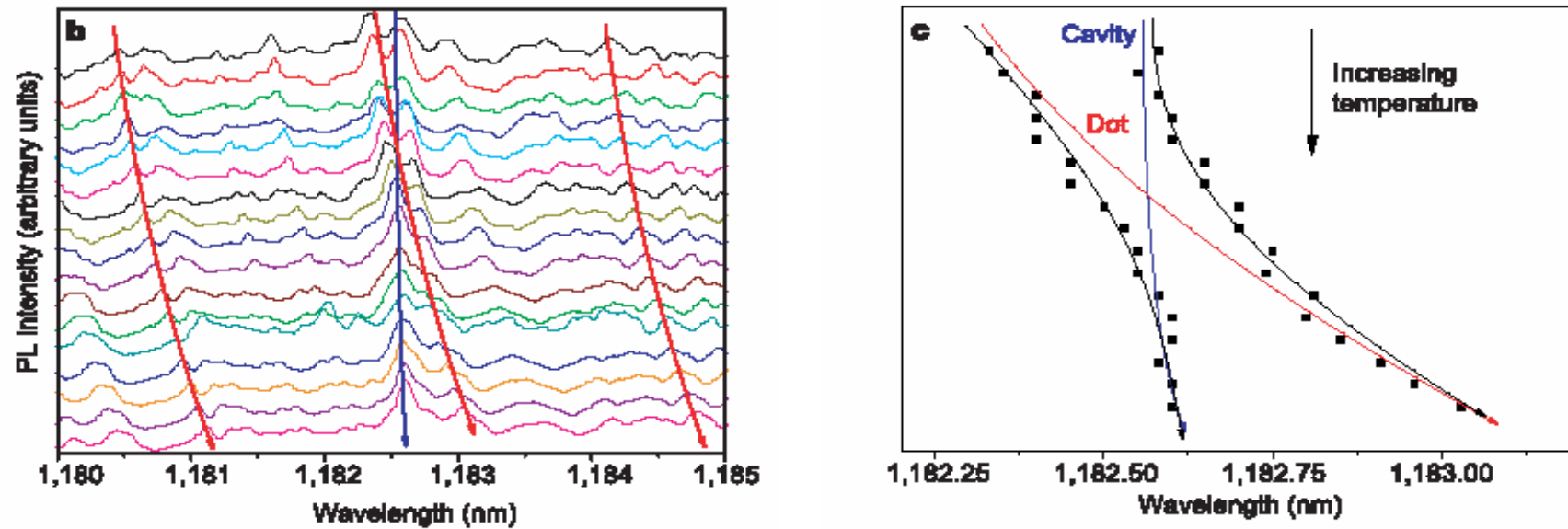


three different
cavities of high Q



Strong coupling for a single InAs QD

Yoshie, Nature 432, 200 (2004)



- evidence for a single InAs QD in the strong coupling regime : $\Omega_R \sim 170 \mu\text{eV}$
- strong coupling also obtained (**simultaneously !!**) for
 - a single InGaAs QD in **micropillar** Reithmaier, Nature 432, 197 (2004)
 - a single GaAs QD in **microdisk** Peter (LPN-France), submitted to PRL

